

UT-13-27
July, 2013

Inflationary Gravitational Waves and the Evolution of the Early Universe

Ryusuke Jinno, Takeo Moroi and Kazunori Nakayama

Department of Physics, University of Tokyo, Tokyo 113-0033, Japan

Abstract

We study the effects of various phenomena which may have happened in the early universe on the spectrum of inflationary gravitational waves. The phenomena include phase transitions, entropy productions from non-relativistic matter, the production of dark radiation, and decoupling of dark matter/radiation from thermal bath. These events can create several characteristic signatures in the inflationary gravitational wave spectrum, which may be direct probes of the history of the early universe and the nature of high-energy physics.

arXiv:1307.3010v2 [hep-ph] 22 Jul 2013

Contents

1	Introduction	2
2	Basic properties of GWs	3
2.1	Background Evolution	3
2.2	Evolution of GWs: case without dark radiation	4
2.2.1	Evolution equation	4
2.2.2	GW spectrum: modes entering the horizon at the RD era	5
2.2.3	GW spectrum: modes entering the horizon at the non-RD era	5
2.3	Evolution of GWs: effects of dark radiation	6
2.3.1	Evolution equation	6
2.3.2	Overall normalization	6
3	Illustration with simple examples	9
3.1	Phase transition	9
3.2	Entropy production	10
3.3	Phase transition and dark radiation	11
3.4	Entropy production and dark radiation	13
3.5	Decay of dark radiation into visible radiation	13
4	Examples of the GW spectrum	15
4.1	Case 1	15
4.2	Case 2	17
4.3	Case 3	19
4.4	Case 4	21
4.5	Case 5	23
5	Model	24
5.1	SUSY Peccei-Quinn model	26
5.2	SUSY majoron model	33
6	Conclusions	35
A	Inflationary GW power spectrum	35
B	GW spectrum with a brief period of inflation	39
B.1	GW spectrum with brief period of inflation	39
B.2	Oscillations in the GW spectrum	41
B.2.1	The reason for the oscillations in the GW spectrum	42
B.2.2	Oscillation period	42

1 Introduction

The early universe is a good laboratory for high-energy physics because the temperature can be much higher than the reach of the accelerator experiments. Thus we may be able to probe high-energy physics by observing some relics of the hot early universe. The anisotropy of the cosmic microwave background (CMB) carries rich information on the primordial density perturbation, which is considered to be generated during inflationary era. Hence the precise observation of CMB gives a clue to inflation models; it is a great success of cosmology for probing high-energy physics.

However, it is rather unknown what have happened in the era between the inflation and the big-bang nucleosynthesis (BBN). To go beyond, one of the promising such relics that carry direct information on the early universe is the gravitational waves (GWs), since GWs propagate without interfered by matter and radiation. In this paper, we focus on inflationary GWs as a possible probe of the early universe.

The early universe may have experienced several drastic phenomena, which are not expected in the standard model (SM), e.g., phase transitions, entropy productions, production of weakly-interacting particles, etc. It is known that the spectrum of inflationary GWs reflects the equation of state of the early universe as studied in Refs. [1, 2, 3, 4, 5, 6, 7, 8, 9, 10, 11, 12, 13, 14]. In particular, it is possible to determine or constrain the reheating temperature of the universe [9, 10, 13] with future space laser interferometers [15, 16, 17]. If there is a brief period of inflation (other than the one responsible for the present density perturbations) such as thermal inflation [18, 19], the spectrum exhibits a characteristic feature [20]. The effects of very weakly interacting relativistic particles, or dark radiation, on the GW spectrum were pointed out in Refs. [21, 22, 23, 24, 25]. In the presence of decaying matter into dark radiation, the GW spectrum is deformed in a nontrivial way [25].

In a realistic setup, the GW spectrum would be affected in a complicated way. For example, in the Peccei-Quinn (PQ) model for solving the strong CP problem [26, 27], the PQ phase transition may have occurred at around the cosmic temperature $T \sim 10^9\text{--}10^{12}$ GeV, and huge amount of entropy could have been released in association with the phase transition. Relativistic axions may have been also efficiently produced by the decay of the PQ scalar condensate, which would contribute as dark radiation. All these phenomena significantly affect the spectrum of inflationary GWs. In other words, it may be possible to access the high-energy phenomena and underlying physical processes by studying the detailed spectrum of inflationary GWs.

In this paper we study the inflationary GW spectrum in detail in various setups having concrete models in mind. The combinations of above mentioned effects make several characteristic features in the spectra, which enable us to infer information on the early universe phenomena.

First we review basic properties of GWs in Sec. 2, including the GW spectrum and effects of the anisotropic stress. In Sec. 3, we exhibit some simple examples of the GW spectrum as a first step to the following section. In Sec. 4, we combine all these effects to show the realistic GW spectra with several typical examples. In Sec. 5 particle physics motivated

models will be provided in which the GW spectrum actually becomes complicated. Sec. 6 is devoted to conclusions.

2 Basic properties of GWs

2.1 Background Evolution

Before discussing the evolution of GWs we first explain that of background, which we assume throughout this paper to be the Friedmann-Robertson-Walker (FRW) universe with negligible curvature. The FRW metric and its tensor perturbation are given by

$$ds^2 = -dt^2 + a^2(t)(\delta_{ij} + h_{ij}(t, \mathbf{x}))dx^i dx^j, \quad (2.1)$$

where $a(t)$ is the scale factor and $h_{ij} = h_{ji}$ satisfies transverse and traceless condition: $h_{ii} = h_{ij,i} = 0$.

The evolution of the FRW universe is described by the Friedmann equation

$$H^2 = \frac{8\pi G}{3}\rho_{\text{tot}} = \frac{1}{3M_P^2}\rho_{\text{tot}}, \quad (2.2)$$

where $H = \dot{a}/a$, and $M_P \simeq 2.4 \times 10^{18}\text{GeV}$ is the reduced Planck mass. The total energy density of the universe, ρ_{tot} , generally include

$$\rho_{\text{tot}} = \rho_{\text{vac}} + \rho_{\text{m}} + \rho_{\text{r}} + \rho_X, \quad (2.3)$$

where ρ_{vac} , ρ_{m} , ρ_{r} and ρ_X represent the vacuum, matter, (visible) radiation and dark radiation energy densities, respectively.^{#1} The radiation energy density ρ_{r} is related to the cosmic temperature T as

$$\rho_{\text{r}} = \frac{\pi^2}{30}g_*T^4, \quad (2.4)$$

where g_* is the relativistic degrees of freedom. Unless otherwise stated, we use $g_* = 228.75$, which is the value in the minimal supersymmetric (SUSY) standard model (MSSM) at high enough temperature.^{#2} The amounts of other components depend on the particle physics model and there can be energy transfers among these components. Thus the Hubble expansion rate reflects their behavior in the early universe and it directly affects the GW spectrum as shown below. We will study concrete setups in the following sections.

^{#1}In this paper, we call the energy density with $w = -1$ (with w being the equation-of-state parameter) “vacuum energy.”

^{#2}Including other fields than in MSSM causes deviation from this value, but we neglect it as small.

2.2 Evolution of GWs: case without dark radiation

2.2.1 Evolution equation

Substituting the metric Eq. (2.1) into the Einstein equation, we get the equation of motion of GWs:

$$\ddot{h}_{ij} + 3H\dot{h}_{ij} - \frac{\nabla^2}{a^2}h_{ij} = 16\pi G\Pi_{ij}, \quad (2.5)$$

where Π_{ij} is the anisotropic stress of the energy-momentum tensor, which satisfies $\Pi_{ii} = \Pi_{ij,i} = 0$. We decompose h_{ij} using polarization tensors $e_{ij}^{+, \times}$,

$$h_{ij}(t, \mathbf{x}) = \sum_{\lambda=+, \times} \int \frac{d^3k}{(2\pi)^3} h(t, \mathbf{k}, \lambda) e^{i\mathbf{k}\cdot\mathbf{x}} e_{ij}^\lambda, \quad (2.6)$$

to rewrite Eq. (2.5) into

$$\ddot{h}(t, \mathbf{k}, \lambda) + 3H\dot{h}(t, \mathbf{k}, \lambda) + \frac{k^2}{a^2}h(t, \mathbf{k}, \lambda) = 16\pi G\Pi(t, \mathbf{k}, \lambda). \quad (2.7)$$

Here $k = |\mathbf{k}|$, and we have performed the same decomposition and transformation on Π_{ij} as is done on h_{ij} . Also, we define the polarization tensors so that they satisfy $e_{ij}^\lambda = e_{ji}^\lambda$, $e_{ii}^\lambda = e_{ij,i}^\lambda = 0$ and $e_{ij}^\lambda e_{ij}^{\lambda'*} = \delta_{\lambda\lambda'}$.

For later use, we introduce the variable u defined by

$$u = k\eta = k \int_0^t \frac{dt'}{a(t')}, \quad (2.8)$$

and rewrite Eq. (2.7) to get

$$h''(u, \mathbf{k}, \lambda) + 2H_u h'(u, \mathbf{k}, \lambda) + h(u, \mathbf{k}, \lambda) = 16\pi G \left(\frac{a}{k}\right)^2 \Pi(u, \mathbf{k}, \lambda), \quad (2.9)$$

where the prime denotes the derivative with respect to u and $H_u \equiv a'/a$. If $a(t) \propto t^p$ as in the radiation dominated (RD) era ($p = 1/2$) or the matter-dominated (MD) era ($p = 2/3$), we obtain $u = \frac{p}{1-p} \frac{k}{aH}$. Imposing the initial condition of $h(t, \mathbf{k}, \lambda) \rightarrow h_{\text{prim}}(\mathbf{k}, \lambda)$ for $t \rightarrow 0$, the solution of Eq. (2.9), when the anisotropic stress is neglected, is given by

$$h(u, \mathbf{k}, \lambda) = h_{\text{prim}}(\mathbf{k}, \lambda) j_0(u) \quad \text{for RD}, \quad (2.10)$$

and

$$h(u, \mathbf{k}, \lambda) = h_{\text{prim}}(\mathbf{k}, \lambda) \frac{3j_1(u)}{u} \quad \text{for MD}, \quad (2.11)$$

where j_i are the i -th spherical Bessel function:

$$j_0(u) = \frac{\sin(u)}{u}, \quad j_1(u) = \frac{\sin(u) - u \cos(u)}{u^2}. \quad (2.12)$$

From this solution, it is easily seen that $h(u, \mathbf{k}, \lambda) \sim \text{const.}$ for the modes outside the horizon ($k \ll aH$) and $h(u, \mathbf{k}, \lambda) \propto a^{-1}$ for the modes inside the horizon ($k \gg aH$).

2.2.2 GW spectrum: modes entering the horizon at the RD era

Here we define basic quantities used in the following sections. The energy density of the GWs is given by (see Appendix A for details)

$$\rho_{\text{GW}}(t) = \int d \ln k \rho_{\text{GW}}(t, k) = \frac{1}{32\pi G} \langle h^{ij;0} h_{ij;0} \rangle_{\text{osc}}, \quad (2.13)$$

where $\rho_{\text{GW}}(t, k)$ denotes the energy density of tensor perturbation per logarithmic frequency. In addition, $\langle \dots \rangle_{\text{osc}}$ denotes the oscillation average (and hence the above expression is relevant only for the sub-horizon mode). Taking the ensemble average, we obtain

$$\rho_{\text{GW}}(t, k) = \frac{1}{32\pi G} \frac{k^2}{a^2} \frac{k^3}{2\pi^2} P_h(t, k), \quad (2.14)$$

where P_h is the power spectrum of GWs. The GW spectrum $\Omega_{\text{GW}}(t, k)$ is defined as

$$\Omega_{\text{GW}}(t, k) \equiv \frac{\rho_{\text{GW}}(t, k)}{\rho_{\text{tot}}(t)}. \quad (2.15)$$

For the GW modes entering the horizon at the RD era, the present value of Ω_{GW} is evaluated as

$$\Omega_{\text{GW}}(t_0, k) \simeq 7.9 \times 10^{-15} \left(\frac{g_*(T_{\text{hi}})}{g_*(T_{\text{eq}})^{\text{(std)}}} \right) \left(\frac{g_{*s}(T_{\text{eq}})}{g_{*s}(T_{\text{hi}})} \right)^{4/3} \left(\frac{k}{k_0} \right)^{n_t} r, \quad (2.16)$$

where r is the tensor-to-scalar ratio, T_{eq} is the temperature at the matter-radiation equality.^{#3} (Here, we assume that there is no entropy production after the horizon entry.) Ω_{GW} is weakly dependent on k through $T_{\text{hi}}(k)$ and the tensor spectral index n_t . The relation between the present frequency of GWs and the temperature of the universe at which the corresponding mode entered the horizon is given by

$$f = \frac{k}{2\pi} \simeq 3.0 \text{ Hz} \left(\frac{T}{10^8 \text{ GeV}} \right) \left(\frac{g_*(T)}{228.75} \right)^{1/6}. \quad (2.17)$$

Since future space-based GW detectors are most sensitive to the GW with frequency around 0.1–1 Hz, we can probe the early universe physics with very high temperature through the GW observations.

2.2.3 GW spectrum: modes entering the horizon at the non-RD era

In the above, we have assumed the RD universe at the horizon entry of GWs. This is not guaranteed in general in the early universe where various forms of fluid can dominate the

^{#3} Since at least two species of neutrinos have masses and non-relativistic at present, we use g_* at $T = T_{\text{eq}}$ rather than that at $T = T_0$ (present temperature) to avoid confusion. At $T = T_{\text{eq}}$, all neutrinos are relativistic. See also Appendix A.

energy density. Let us suppose that the universe has the equation of state $w (> -1/3)$, the ratio of the energy density to the pressure, at the horizon entry of GWs. Then the GW spectrum scales as

$$\Omega_{\text{GW}}(t_0, k) \propto k^{\frac{2(3w-1)}{3w+1}}. \quad (2.18)$$

In the MD universe ($w = 0$), $\Omega_{\text{GW}}(t_0, k) \propto k^{-2}$.

If there is a short period of inflation, the expression is a bit complicated. Let us suppose that the equation of state changes as $w_1 \rightarrow w_2 \rightarrow w_3$ with $w_1, w_3 > -1/3$ and $w_2 < -1/3$. The calculation is done in Appendix B and the result is

$$\Omega_{\text{GW}}(t_0, k) \propto k^{2 - \frac{4}{3w_1+1} + \frac{4}{3w_2+1} - \frac{4}{3w_3+1}}. \quad (2.19)$$

for the modes entering the horizon at the intermediate regime. If $w_1 = w_3 = 1/3$ and $w_2 = -1$, we obtain $\Omega_{\text{GW}}(t_0, k) \propto k^{-4}$. If $w_1 = 1/3, w_3 = 0$ and $w_2 = -1$, we obtain $\Omega_{\text{GW}}(t_0, k) \propto k^{-6}$.

2.3 Evolution of GWs: effects of dark radiation

2.3.1 Evolution equation

In the presence of relativistic particles with weak or no interaction, the RHS of Eq. (2.9) does not vanish and affects the evolution of GWs [21, 22, 23, 24, 25]. Let us consider “dark radiation” X , non-interacting relativistic particles, contributing to the anisotropic stress.^{#4} The RHS of Eq. (2.9) is written as an integration including the metric perturbation $h(u, \mathbf{k}, \lambda)$ (see Ref. [25] for derivation),

$$h''(u) + 2H_u h'(u) + h(u) = -24 \left[H_u^2 \frac{1}{a^4 \rho_{\text{tot}}} \right] (u) \int_0^u du' \left[a^4 \rho_X \frac{\partial h}{\partial u} \right] (u') \frac{j_2(u-u')}{(u-u')^2}, \quad (2.20)$$

where ρ_X is the energy density of X , and $j_2(u) = [(3-u^2)\sin(u) - 3u\cos(u)]/u^3$. Also, we have omitted trivial indices. The right-hand side of Eq. (2.20) is due to the backreaction of dark radiation on GWs with kernel $j_2(u)/u^2$. Note that $j_2(u)/u^2$ is suppressed when $u \gg 1$ while $h'(u) \simeq 0$ at $u \ll 1$, hence the anisotropic stress affects the evolution of GWs only around $u \sim 1$, i.e., around the horizon entry in the RD or MD universe.

2.3.2 Overall normalization

The presence of non-interacting particle X at the time of horizon entry or the last-scattering causes a change in the overall normalization of the GW spectrum as shown in Ref. [25]. Here we briefly repeat the result of Ref. [25].

^{#4}We call non-interacting relativistic degrees of freedom at the time of our interest as “dark radiation.” Thus, the dark radiation in our discussion may be massive, and may not correspond to the dark radiation in the present universe.

First, the amount of dark radiation is written in terms of the effective neutrino species N_{eff} as

$$\rho_\nu + \rho_X = N_{\text{eff}} \frac{7}{8} \left(\frac{4}{11} \right)^{4/3} \rho_\gamma, \quad (2.21)$$

where ρ_ν and ρ_γ are the energy densities of the neutrino and photon, respectively. With a standard matter content one expects $N_{\text{eff}}^{(\text{SM})} = 3.046$, and we define

$$\Delta N_{\text{eff}} = N_{\text{eff}} - N_{\text{eff}}^{(\text{SM})}. \quad (2.22)$$

The dependence of $\Omega_{\text{GW}}(t_0, k)$ on ΔN_{eff} comes from g_* and g_{*s} in Eq. (2.16),

$$\Omega_{\text{GW}}(t_0, k) \propto \Omega_{\text{r},0} \gamma \propto g_*(T_0) \gamma, \quad \gamma \equiv \left(\frac{g_*(T_{\text{hi}})}{g_*(T_{\text{eq}})} \right) \left(\frac{g_{*s}(T_{\text{eq}})}{g_{*s}(T_{\text{hi}})} \right)^{4/3}. \quad (2.23)$$

Then, we obtain

$$\gamma = \frac{1 + \frac{7}{43} \left(\frac{g_{*s}(T_{\text{hi}})}{10.75} \right)^{1/3} \Delta N_{\text{eff}}}{1/\gamma^{(\text{std})} + \frac{7}{43} \left(\frac{g_{*s}(T_{\text{hi}})}{10.75} \right)^{1/3} \Delta N_{\text{eff}}}, \quad (2.24)$$

where, here and hereafter, the superscript “(std)” is for quantities in the case without dark radiation (i.e., $\Delta N_{\text{eff}} = 0$). Also, the relation between $g_*(T_{\text{eq}})$ and $g_*^{(\text{std})}(T_{\text{eq}})$ is

$$\frac{g_*(T_{\text{eq}})}{g_*^{(\text{std})}(T_{\text{eq}})} = \frac{2 \left[1 + N_{\text{eff}} \cdot \frac{7}{8} \cdot \left(\frac{4}{11} \right)^{4/3} \right]}{2 \left[1 + N_{\text{eff}}^{(\text{std})} \cdot \frac{7}{8} \cdot \left(\frac{4}{11} \right)^{4/3} \right]}. \quad (2.25)$$

Then we define the overall factor C_1 as

$$C_1 \equiv \frac{g_*(T_{\text{eq}})}{g_*^{(\text{std})}(T_{\text{eq}})} \frac{\gamma}{\gamma^{(\text{std})}}, \quad (2.26)$$

which is plotted in Fig. 1.

This C_1 factor is partially compensated by the effect of anisotropic stress caused by X . If X exists before the horizon entry, the RHS of Eq. (2.20) can be simplified as [21]

$$\text{RHS of Eq. (2.20)} = -24[H_u^2 f_X](u) \int_0^u du' \frac{\partial h}{\partial u}(u') \frac{j_2(u-u')}{(u-u')^2}, \quad (2.27)$$

where $f_X = \rho_X/\rho_{\text{tot}}$ is the energy fraction of X . In this case, assuming the RD universe, the suppression of GW spectrum caused by X is calculated analytically. The suppression factor is defined as^{#5}

$$C_3 \equiv \frac{\Omega_{\text{GW}} \big|_{\text{w/ stress}}}{\Omega_{\text{GW}} \big|_{\text{w/o stress}}}, \quad (2.28)$$

^{#5}The notations C_1 and C_3 follow those of Ref. [4].

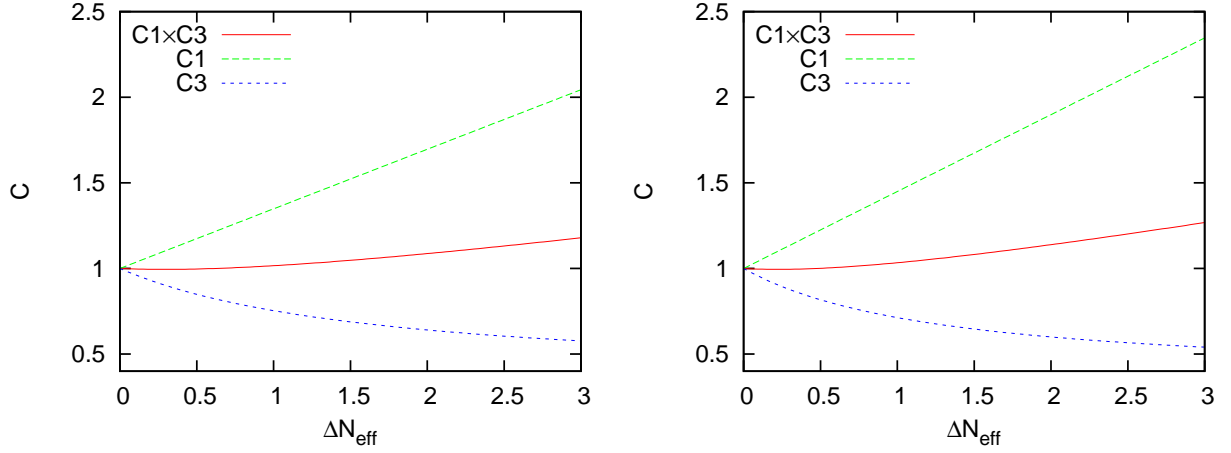


Figure 1: Normalization factor C with the presence of dark radiation. C_1 accounts for the effect of increase in the amount of total radiation, while C_3 gives that of anisotropic stress due to the dark radiation. The left figure is for the SM, while the right is for the MSSM.

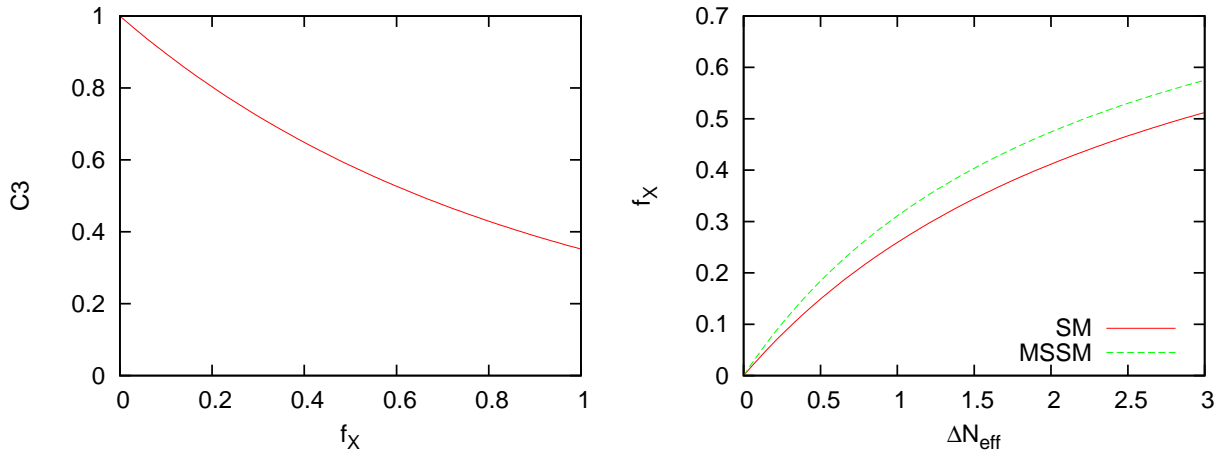


Figure 2: Left : Normalization factor C_3 as a function of f_X , the energy fraction of dark radiation. Right : Relation between the effective neutrino number ΔN_{eff} and f_X .

whose dependence on f_X was analytically derived in Refs. [22, 4] and plotted in Fig. 2. The relation between f_X and ΔN_{eff} is given by

$$f_X = \frac{\frac{7}{4} \left(\frac{4}{43}\right)^{4/3} \left[g_{*s}^{(\text{std})}(T_{\text{hi}})\right]^{3/4} \Delta N_{\text{eff}}}{g_*^{(\text{std})}(T_{\text{hi}}) + \frac{7}{4} \left(\frac{4}{43}\right)^{4/3} \left[g_{*s}^{(\text{std})}(T_{\text{hi}})\right]^{3/4} \Delta N_{\text{eff}}}. \quad (2.29)$$

Then the present GW spectrum reads

$$\Omega_{\text{GW}}(t_0, k) = C_1 C_3 \times \Omega_{\text{GW}}^{(\text{std})}(t_0, k) \quad (2.30)$$

for the mode entering the horizon at the RD era. This gives the overall normalization of the GW spectrum in the low-frequency limit, $k < k_{\text{EW}}$, where k_{EW} is the comoving Hubble scale at around the electroweak phase transition. The total modification on the overall normalization on Ω_{GW} , $C_1 \times C_3$, is plotted in Fig. 1.

In the following sections, we calculate the GW spectrum by using numerical calculation, taking account of the effects of anisotropic stress. However, the normalization related to the C_1 factor is not included in the following calculations because it is model-dependent; C_1 depends whether X remains non-interacting and relativistic until present or not. Thus one should note that Ω_{GW} given in the figures in the following sections should be multiplied by C_1 if the X particle behaves as dark radiation until today.

3 Illustration with simple examples

As we have mentioned, the spectrum of the inflationary GWs is sensitive to the thermal history of the universe. To see basic features of GW spectrum, in this section, we exhibit some simple examples for the GW spectrum modified by the phase transition, entropy production and dark radiation.

3.1 Phase transition

As a first example, let us consider a scalar field ϕ with a symmetry breaking potential, e.g., $V = \lambda(\phi^2 - v^2)^2$. We consider the case where ϕ is trapped at the origin due to thermal effects [20]. If the interaction of ϕ with the particles in thermal bath is strong enough, the vacuum energy dominates the universe, and a brief period of inflation occurs, as in the case of thermal inflation [18, 19]. The phase transition happens after inflation and the subsequent oscillation of the field is assumed to instantly decay into radiation. The background equations we solve are Eq. (2.2) with

$$\rho_{\text{vac}} = \begin{cases} \Lambda^4 & (t < t_{\text{PT}}) \\ 0 & (t > t_{\text{PT}}) \end{cases}, \quad (3.1)$$

$$\dot{\rho}_{\text{r}} + 4H\rho_{\text{r}} = \Lambda^4 \delta(t - t_{\text{PT}}), \quad (3.2)$$

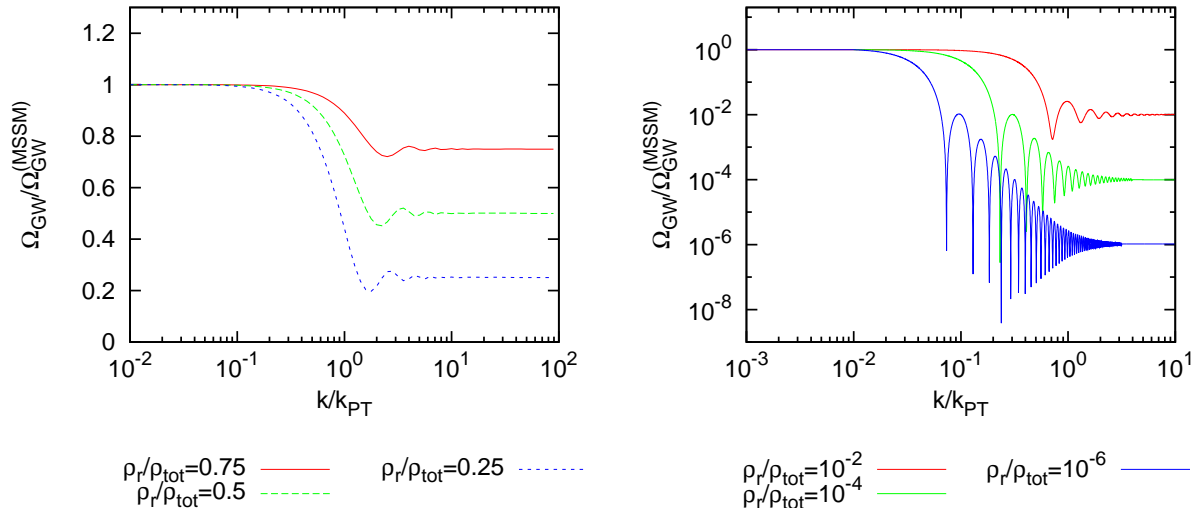


Figure 3: GW spectrum with phase transition and instant decay into radiation. We assumed that the universe is radiation dominated before the vacuum energy dominates it, and varied the ratio of radiation energy density to the total energy density at the phase transition.

where t_{PT} is the cosmic time at the phase transition. We numerically solved these with Eq. (2.9), and the resultant Ω_{GW} is shown in Fig. 3. We varied the ratio of ρ_r to $\rho_{tot} \equiv \rho_r + \rho_{vac}$ at the time of phase transition. The horizontal axis is normalized with k_{PT} , which satisfies $k = aH$ at the phase transition. Note that the ratio of the spectrum in $k \gg k_{PT}$ to that of $k \ll k_{PT}$ is equal to ρ_r/ρ_{tot} just before the phase transition, which is from the fact that $\rho_{GW}(k \gg aH) \propto a^{-4}$. GWs inside the horizon at the phase transition are diluted by the newly-produced radiation, while those outside the horizon remains $h_{ij} = \text{const}$. Note the characteristic oscillatory feature around $k \simeq k_{PT}$. The reason for the oscillatory feature and the oscillation period is explained in Appendix B. Finally, note that in the limit of long duration of thermal inflation, the spectrum scales as $\propto k^{-4}$ as shown also in Appendix B.

3.2 Entropy production

Next we consider the case of late-time entropy production, i.e., the case where some matter dominates universe, and then it decays into radiation. The background equations we solve are Eq. (2.2) and

$$\dot{\rho}_m + 3H\rho_m = -\Gamma\rho_m, \quad (3.3)$$

$$\dot{\rho}_r + 4H\rho_r = \Gamma\rho_m, \quad (3.4)$$

where Γ is the decay rate of the non-relativistic matter. The result is shown in Fig. 4. We varied the ratio of ρ_r to $\rho_{tot} \equiv \rho_r + \rho_m$ at the decay. The horizontal axis is normalized with

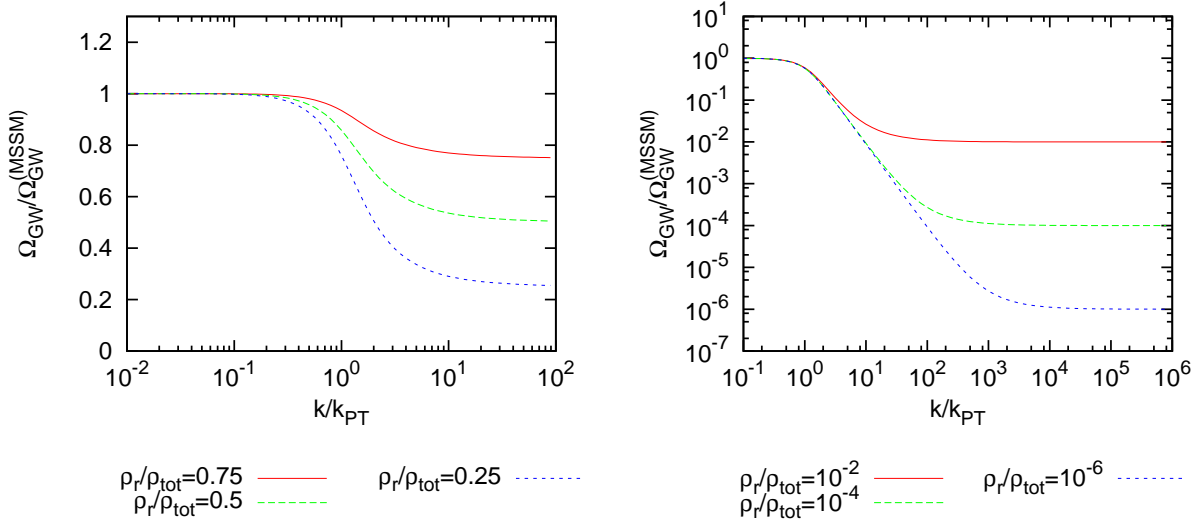


Figure 4: GW spectrum with entropy injection. We varied the ratio of radiation energy density to the total energy density at $t = t_{\text{dec}} \equiv \Gamma^{-1}$.

k_{decay} , which is defined as the comoving Hubble scale aH at $t = \Gamma^{-1}$. Note that the ratio of the spectrum in $k \gg k_{\text{decay}}$ to that of $k \ll k_{\text{decay}}$ is equal to ρ_r/ρ_{tot} at the decay for the same reason written in the previous subsection. In this case the spectrum scales as $\propto k^{-2}$ for the mode entering the horizon at the non-relativistic matter dominated era. Also note that there is no oscillatory feature in the GW spectrum in contrast to the previous case.

3.3 Phase transition and dark radiation

Let us consider the case where vacuum energy of a scalar field dominates the universe as in the case of Sec. 3.1, but at a certain time the energy is instantly converted to dark radiation X . We numerically solved the Friedmann equation Eq. (2.2) with

$$\rho_{\text{vac}} = \begin{cases} \Lambda^4 & (t < t_{\text{PT}}) \\ 0 & (t > t_{\text{PT}}) \end{cases}, \quad (3.5)$$

$$\dot{\rho}_r + 4H\rho_r = 0, \quad (3.6)$$

$$\dot{\rho}_X + 4H\rho_X = \Lambda^4\delta(t - t_{\text{PT}}). \quad (3.7)$$

Then we expect the following features in the GW spectrum:

- For large wavenumber $k \gg k_{\text{PT}}$, there is the same suppression as Fig. 3.
- For small wavenumber $k \ll k_{\text{PT}}$, there is a suppression due to the anisotropic stress, caused by the RHS of Eq. (2.20).

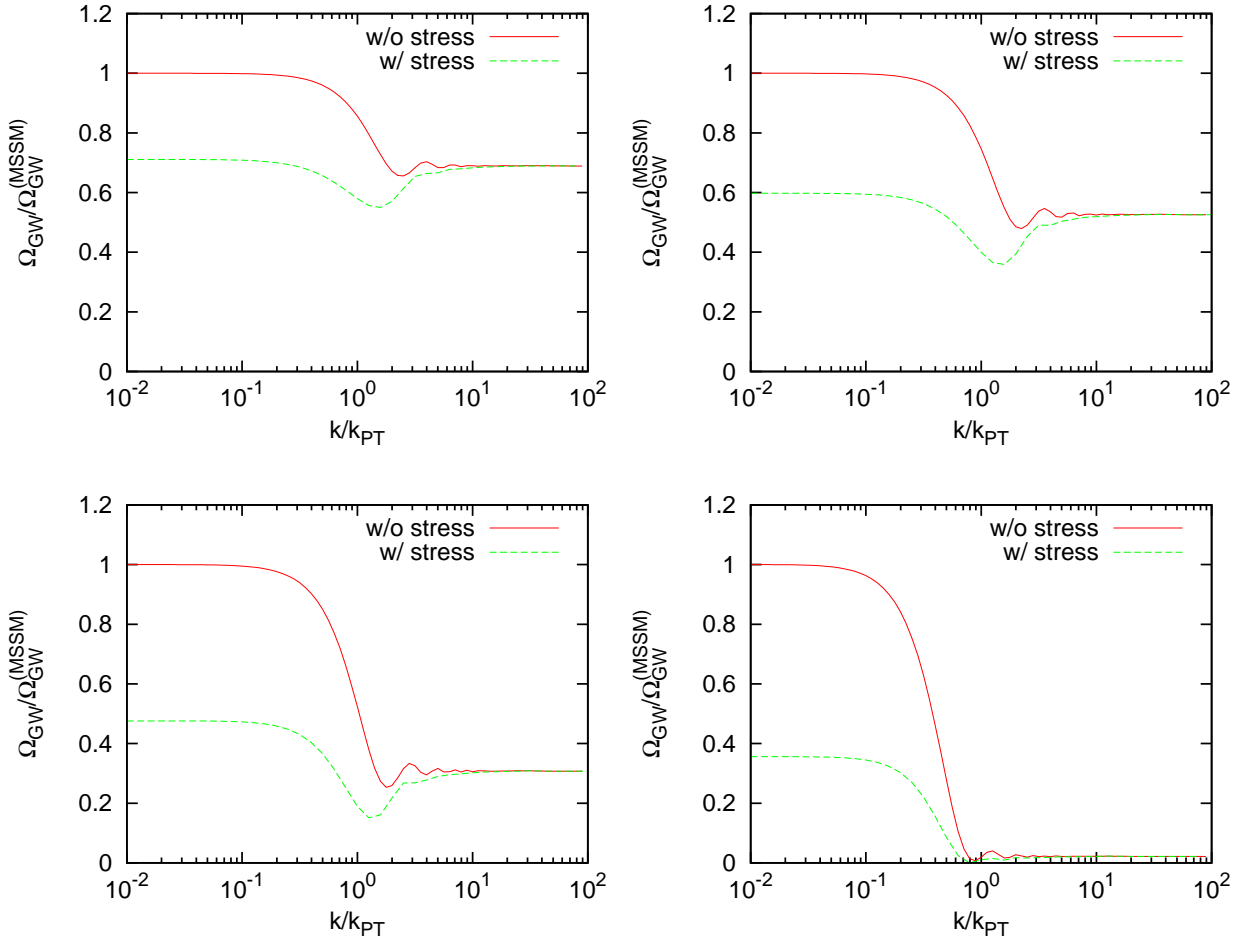


Figure 5: GW spectrum with phase transition and subsequent instant decay into dark radiation X . We have assumed that the branching ratio to X is 0 and 1 in the red-solid and green-dashed line, respectively. Also, $\Delta N_{\text{eff}} = 1, 2, 5$ and 100 for the top left, top right, bottom left and bottom right figure, respectively.

The reason for no suppression by the anisotropic stress at $k \gg k_{\text{PT}}$ is that, for GWs of such large wavenumber, there do not exist X particles at the time of their horizon entry. The results of numerical calculations are shown in Fig. 5. In the figure we varied Λ so that ΔN_{eff} (after the phase transition) becomes 1, 2, 5 and 100. Note that ΔN_{eff} here is evaluated assuming that X is relativistic and survives until today. If X decays into radiation at some epoch, or if there exists another entropy production, the X abundance at the epochs of the BBN and radiation-matter equality can be reduced, hence $\Delta N_{\text{eff}} \gg 1$ does not necessarily conflict with observations. In such a case the overall normalization of the GW spectrum changes, but the shape of the spectrum does not change. One sees a dip around $k \simeq k_{\text{PT}}$, which could be a smoking-gun signal of the phase transition followed by the production of dark radiation.

3.4 Entropy production and dark radiation

Next let us consider the case where some massive particle dominates the universe as in the case of Sec. 3.2, but then it decays into dark radiation X [25]. We numerically solved Eq. (2.2) and

$$\dot{\rho}_m + 3H\rho_m = -\Gamma\rho_m, \quad (3.8)$$

$$\dot{\rho}_r + 4H\rho_r = 0, \quad (3.9)$$

$$\dot{\rho}_X + 4H\rho_X = \Gamma\rho_m. \quad (3.10)$$

The results of numerical calculations are shown in Fig. 6. One also sees a characteristic dip around $k \simeq k_{\text{PT}}$ as in the previous case.

3.5 Decay of dark radiation into visible radiation

Another interesting possibility is that X is produced at some time or has existed from the beginning, and then decays into visible radiation while X is still relativistic. In this case the background equations we should solve are

$$\frac{\partial \ln(a^3 F_X)}{\partial t} = H \frac{\partial \ln(a^3 F_X)}{\partial \ln E} - \frac{m\Gamma}{E}, \quad (3.11)$$

$$\dot{\rho}_X + \dot{\rho}_r + 4H(\rho_X + \rho_r) = 0, \quad (3.12)$$

where m is the (small) mass of X , Γ is the decay rate of X and $F_X(t, E)$ is defined so that X with energy $E - E + dE$ carries energy density of $F_X(t, E)dE$ at the time t .^{#6} It satisfies $\int dE F_X(t, E) = \rho_X(t)$. We solved Eq. (2.2), Eq. (2.20), Eq. (3.11), and Eq. (3.12), varying the initial ratio of ρ_X to ρ_r and the energy dependence of F_X . The result is shown in Fig. 7 for the case where the dark radiation initially dominates the universe. We consider three cases

^{#6}Without decay, the energy density carried by X with energy $E - E + dE$ in a comoving volume falls proportional to a^{-1} :

$$a^3(t+dt)F_X(t+dt, E(t+dt))dE(t+dt) = \frac{a(t)}{a(t+dt)}a^3(t)F_X(t, E(t))dE(t).$$

Since we know that $E(t)$, $dE(t) \propto a^{-1}$, we obtain

$$\frac{\partial \ln(a^3 F_X)}{\partial t} - H \frac{\partial \ln(a^3 F_X)}{\partial \ln E} = 0.$$

If we include decay, the energy density decreases with decay rate Γ suppressed by the γ -factor:

$$\begin{aligned} a^3(t+dt)F_X(t+dt, E(t+dt))dE(t+dt) &= \frac{a(t)}{a(t+dt)}a^3(t)F_X(t, E(t))dE(t) \\ &\quad - \frac{\Gamma}{E(t)/m}a^3(t)F_X(t, E(t))dE(t). \end{aligned}$$

Again using $E(t)$, $dE(t) \propto a^{-1}$, we get Eq. (3.11).

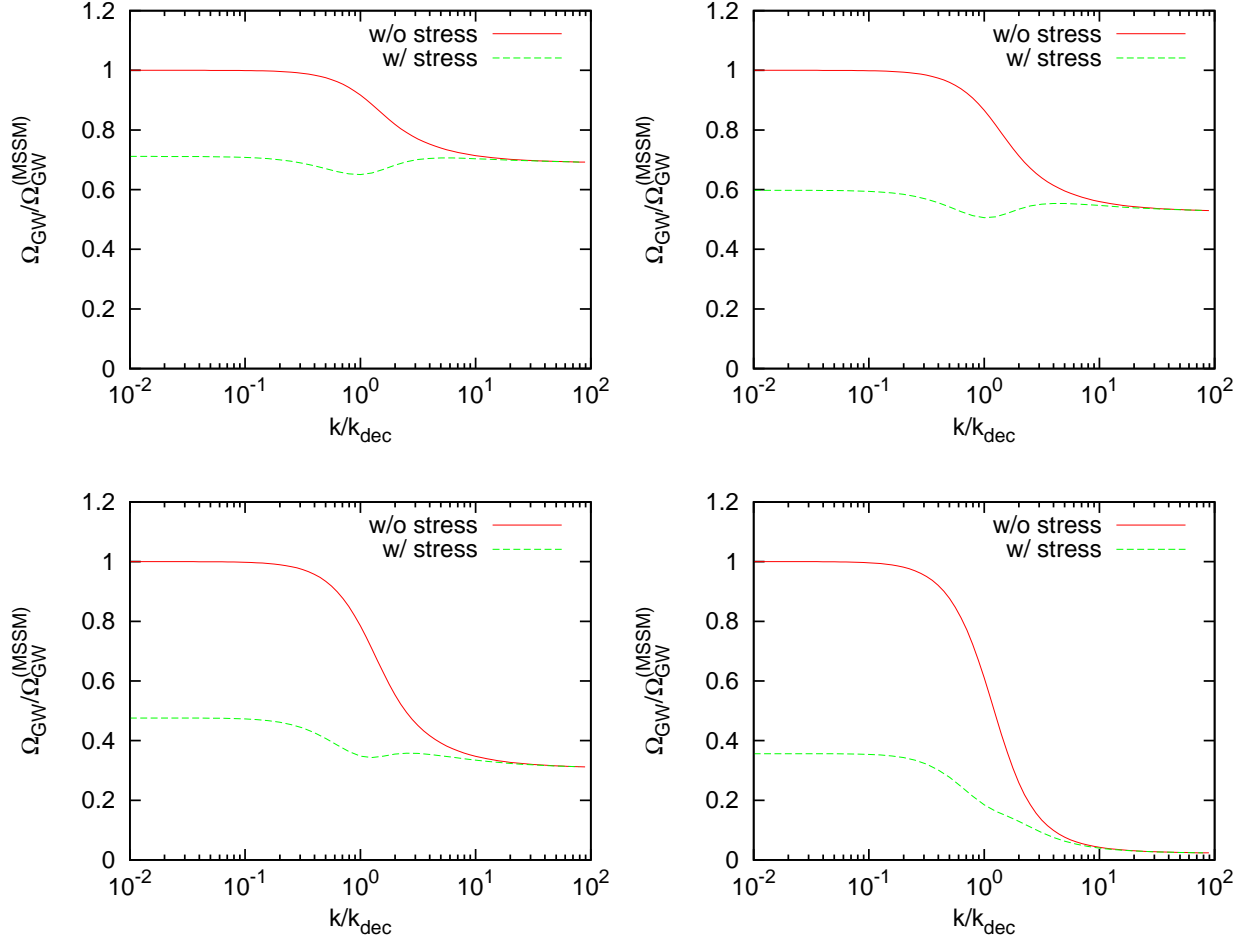


Figure 6: GW spectrum with the decay of massive particle into dark radiation. The horizontal axis is normalized by $k_{\text{dec}} \equiv aH(t = \Gamma^{-1})$, We have assumed that the branching ratio to X is 0 and 1, in the red-solid and green-dashed line, respectively. Also, $\Delta N_{\text{eff}} = 1, 2, 5$ and 100 for the top left, top right, bottom left and bottom right figure, respectively.

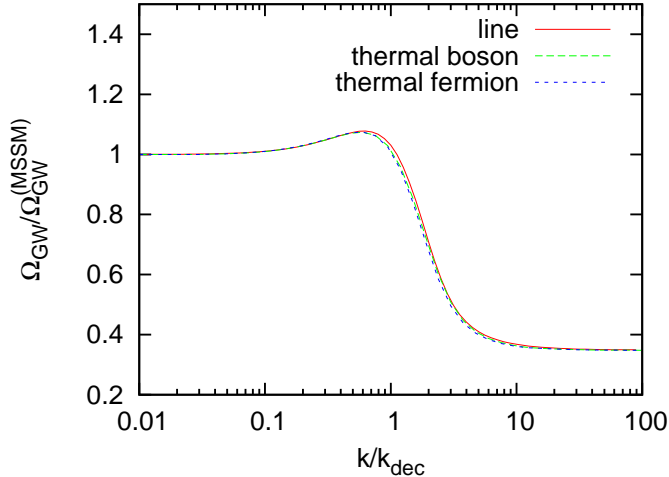


Figure 7: GW spectrum with the decay of dark radiation X into visible radiation. We varied the energy distribution of the dark radiation.

with different distribution functions: the line (i.e., $F_X(t, E) \propto \delta(E_0)$), bosonic, and fermionic thermal distributions. Note that the spectrum has a hill around $k \simeq k_{\text{dec}}$, where k_{dec} for the line distribution is defined as the comoving Hubble scale $k = aH$ at $t = (m\Gamma/E)^{-1}$. For thermal distribution it is defined as $k = aH$ at $t = (m\Gamma/\tilde{E})^{-1}$ with $\tilde{E} \simeq T$. We found no significant differences in the GW spectrum among these distributions. Thus, in studying the relativistic decay of dark radiation in the next section, we approximate that it has the line spectrum.

4 Examples of the GW spectrum

In this section we study the spectrum of the GW in cases with the combinations of events discussed in the previous section, which may be realized in some models motivated by particle physics. (See the flow chart given in Fig. 8.) In our study, we perform the analysis as general as possible, without specifying underlying models. Examples of particle-physics models realizing the scenarios in this section will be discussed in the next section.

4.1 Case 1

In this subsection we assume that the universe has undergone the following events in a time ordering:

1. A brief period of thermal inflation is caused by a scalar field ϕ .
2. After the phase transition, ϕ instantaneously decays into radiation with short mean free path.

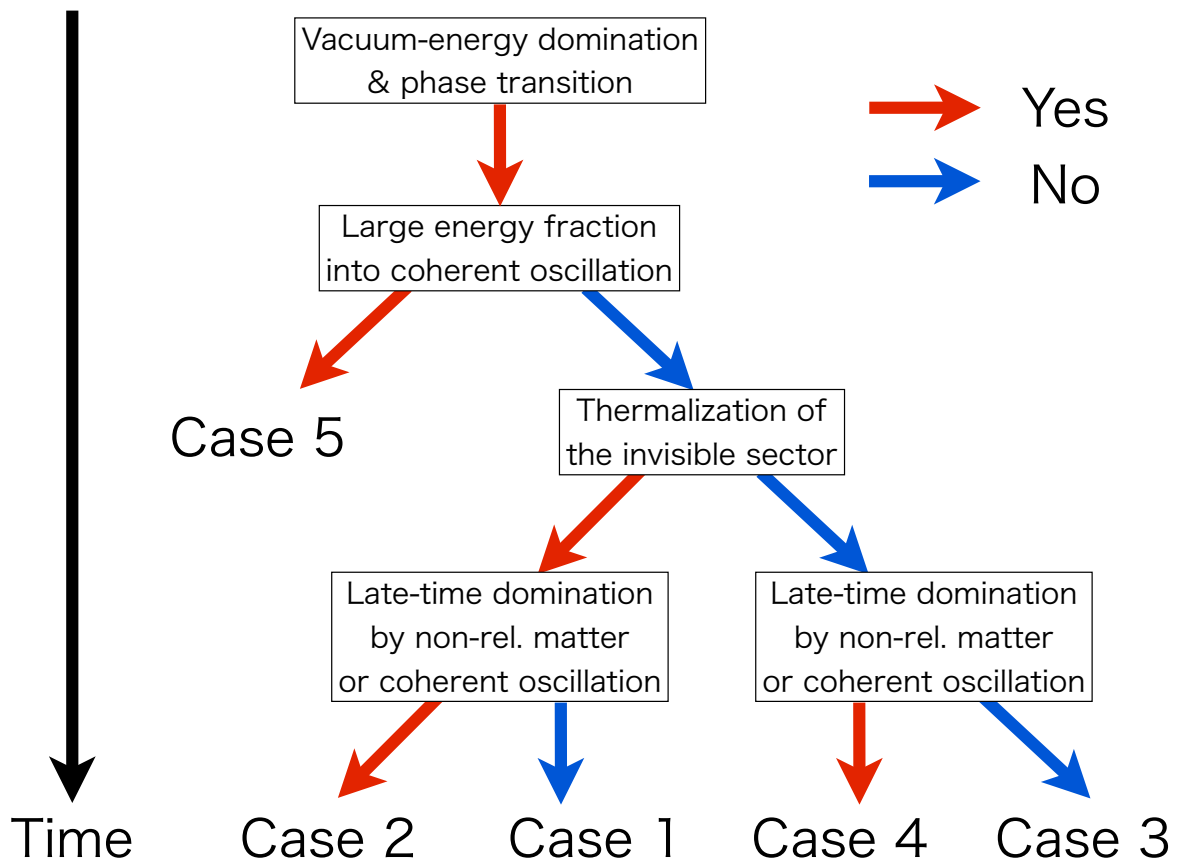


Figure 8: The Cases discussed in this paper.

3. X particles decouple from the thermal bath, after which X particles behave as dark radiation.
4. Part of the decoupled particles X decays into visible radiation.

Before thermal inflation, the universe is assumed to be radiation dominated. Each component evolves as

$$\rho_{\text{vac}} = \begin{cases} \Lambda^4 & \text{for } t < t_{\text{PT}} \\ 0 & \text{for } t > t_{\text{PT}}, \end{cases} \quad (4.1)$$

$$\dot{\rho}_{\text{r}} + 4H\rho_{\text{r}} = \Lambda^4\delta(t - t_{\text{PT}}) - \epsilon_X\rho_{\text{r}}\delta(t - t_{\text{decouple}}) + \frac{m}{E}\Gamma\rho_{X_1}, \quad (4.2)$$

$$\dot{\rho}_{X_1} + \left(4H + \frac{m}{E}\Gamma\right)\rho_{X_1} = \epsilon_{X_1}\rho_{\text{r}}\delta(t - t_{\text{decouple}}), \quad (4.3)$$

$$\dot{\rho}_{X_2} + 4H\rho_{X_2} = \epsilon_{X_2}\rho_{\text{r}}\delta(t - t_{\text{decouple}}), \quad (4.4)$$

where $\epsilon_X (= \epsilon_{X_1} + \epsilon_{X_2})$ is the fraction of the radiation which becomes dark radiation X . For simplicity, the decoupling is assumed to occur instantaneously. Dark radiation X is divided into two components X_1 and X_2 , the former of which decays into the radiation in the visible sector. Both X_1 and X_2 contribute to the anisotropic stress, RHS of Eq. (2.20).

The result of numerical calculation on the GW spectrum is shown in Fig. 9. Here, we consider the case where all the vacuum energy eventually goes into X particles which initially have short mean free path. Here, we used $\rho_{\text{r}}/\rho_{\text{tot}} = 0.63$ at the phase transition. We have also taken

$$T_{\text{decouple}} = 10^{-2} \times T_{\text{PT}}, \quad (4.5)$$

$$T_{\text{decay}} = 10^{-4} \times T_{\text{PT}}, \quad (4.6)$$

to fix t_{decouple} and t_{decay} , where T_{decay} is defined as $H(T = T_{\text{decay}}) = m\Gamma/T_{\text{decay}}$. Here m is the mass of X and Γ is the decay rate of X at rest. We have assumed $\epsilon_{X_1} = \epsilon_{X_2} = \epsilon_X/2$ and also fixed ϵ_X so that ΔN_{eff} becomes 0.5.

It is seen that the spectrum changes steeply at $k \simeq k_{\text{PT}}$ due to the brief period of inflation. Due to the presence of dark radiation X , there is a suppression caused by the anisotropic stress for $k \lesssim 10^{-2}k_{\text{PT}}$ because GWs with such wavenumber enter the horizon after the decoupling of X . Finally, since a part of X decays into visible radiation, the suppression becomes weaker for GWs with $k \lesssim 10^{-4}k_{\text{PT}}$ which enter the horizon after the X_1 decay.

4.2 Case 2

Now, let us consider the Case 2, which has the following thermal history. (The first three events are the same as in the Case 1.)

1. A brief period of thermal inflation is caused by a scalar field ϕ .
2. After the phase transition, ϕ instantaneously decays into radiation.

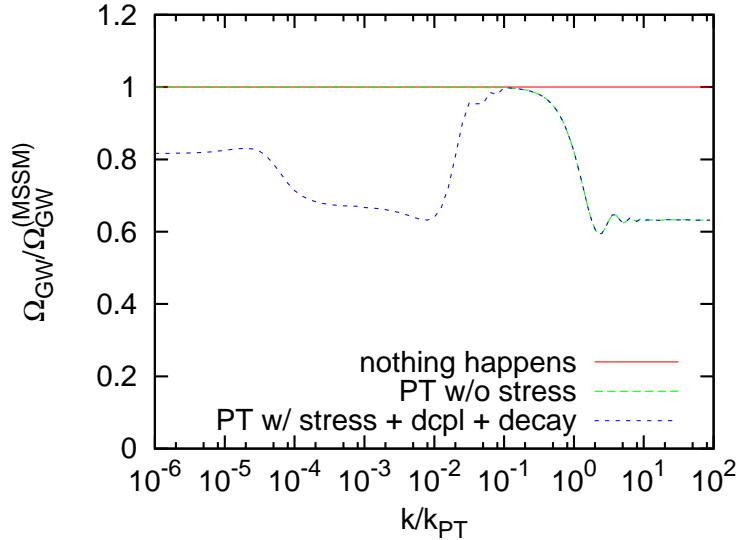


Figure 9: (Blue-dotted) GW spectrum for Case 1, i.e, GW spectrum with decoupling of dark radiation X and subsequent decay of X in addition to the phase transition. ΔN_{eff} is assumed to be 1.3 at the decoupling and then decreases to 0.5 after the decay. (Red-solid) Flat spectrum expected in a simple RD universe. (Green-dashed) GW spectrum for the case without the production of dark radiation.

3. X particles decouple from the thermal bath, after which X particles behave as dark radiation.
4. Some non-relativistic matter begins to dominate the universe.
5. The non-relativistic matter decays into the visible radiation.

Part of visible radiation or X may provide the non-relativistic matter if it becomes non-relativistic due to the redshift. In order to study the case in which the universe evolves from the RD epoch to the MD epoch, we adopt the following equations to follow the evolution of the background:

$$\rho_{\text{vac}} = \begin{cases} \Lambda^4 & \text{for } t < t_{\text{PT}} \\ 0 & \text{for } t > t_{\text{PT}}, \end{cases} \quad (4.7)$$

$$\dot{\rho}_r + 4H\rho_r = \Lambda^4\delta(t - t_{\text{PT}}) - \epsilon_X\rho_r\delta(t - t_{\text{decouple}}) + \Gamma\rho_m, \quad (4.8)$$

$$\dot{\rho}_X + 4H\rho_X = \epsilon_X\rho_r\delta(t - t_{\text{decouple}}), \quad (4.9)$$

$$\dot{\rho}_m + 3H\rho_m = -\Gamma\rho_m, \quad (4.10)$$

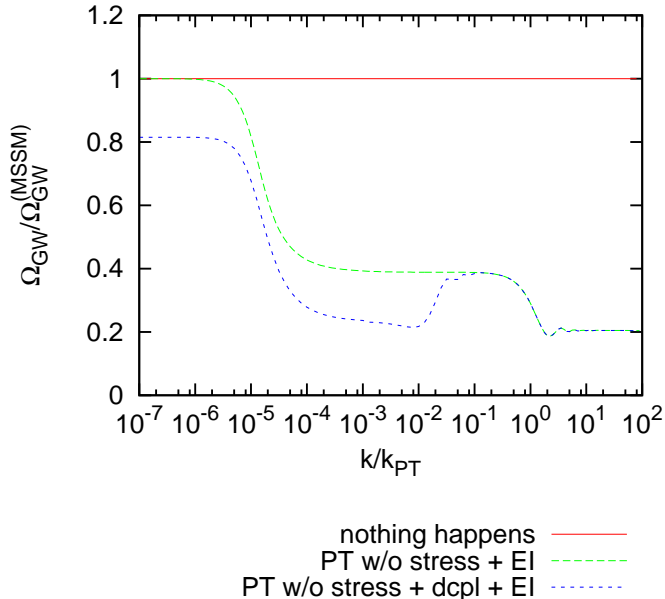


Figure 10: (Blue-dotted) GW spectrum for Case 2; the case with the decoupling of some radiation from thermal bath. ΔN_{eff} is assumed to be 2 at the decoupling and then decrease to 0.5 after decay. (Red-solid) Flat spectrum expected in simple RD universe. (Green-dashed) Spectrum without the production of dark radiation.

where $t_{\text{decouple}} \ll \Gamma^{-1}$. The resulting GW spectra are shown in Fig. 10 and Fig. 11. Here, we assumed instant decoupling as in the Case 1 and

$$T_{\text{decouple}} = 10^{-2} \times T_{\text{PT}}, \quad (4.11)$$

$$T_{\text{decay}} = 10^{-5} \times T_{\text{PT}}. \quad (4.12)$$

In addition, in our calculation, the massive particle which dominates the universe is assumed to originate from the visible radiation. If it is part of the non-interacting radiation we may not apply the derivation of the wave equation in Ref. [25] and the calculation would be very complicated. However, from the fact that massive particles do not generate anisotropic stress, the GW spectrum in such a case is expected to be almost the same in the above figure.

4.3 Case 3

Next, let us consider the following cosmological scenario.

1. A brief period of thermal inflation is caused by a scalar field ϕ .
2. After the phase transition, ϕ instantaneously decays into dark radiation X .
3. Part of dark radiation decays into visible radiation.

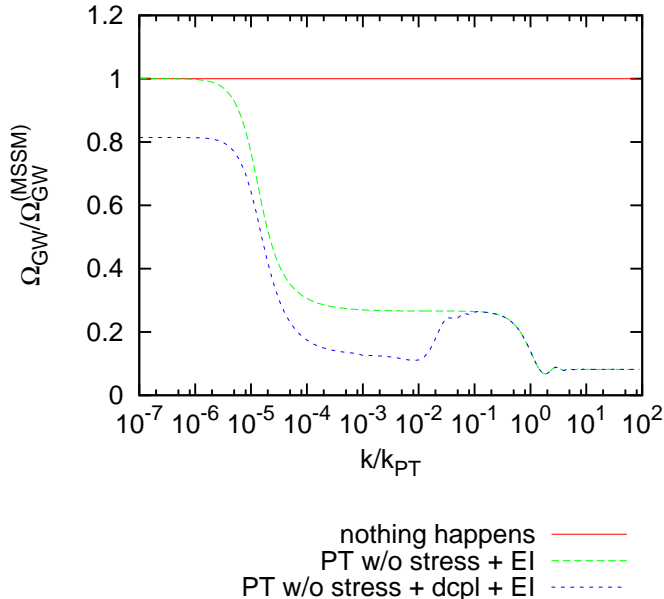


Figure 11: GW spectrum for Case 2. Same as Fig. 10 except that $\Delta N_{\text{eff}} = 5$ at the decoupling.

Here, the decay of ϕ is approximated to occur instantaneously so that dark radiation has monochromatic spectrum (with energy E). Then, each component evolves as

$$\rho_{\text{vac}} = \begin{cases} \Lambda^4 & \text{for } t < t_{\text{PT}} \\ 0 & \text{for } t > t_{\text{PT}}, \end{cases} \quad (4.13)$$

$$\dot{\rho}_{X_1} + 4H\rho_{X_1} = \epsilon_{X_1}\Lambda^4\delta(t - t_{\text{PT}}) - \frac{m\Gamma}{E}\rho_{X_1}, \quad (4.14)$$

$$\dot{\rho}_{X_2} + 4H\rho_{X_2} = \epsilon_{X_2}\Lambda^4\delta(t - t_{\text{PT}}), \quad (4.15)$$

$$\dot{\rho}_r + 4H\rho_r = \frac{m\Gamma}{E}\rho_{X_1}, \quad (4.16)$$

where $\epsilon_{X_1} + \epsilon_{X_2} = 1$. A crucial difference from the previous two cases is that ϕ mainly decays into dark radiation so that the effect of anisotropic stress is already significant just after the phase transition.

The numerical result on the GW spectrum is shown in Fig. 12. We have assumed

$$T_{\text{decay}} = 10^{-2} \times T_{\text{PT}}. \quad (4.17)$$

ϵ_{X_1} and ϵ_{X_2} are chosen so that ΔN_{eff} becomes 1.3 at the decoupling and then decreases to 0.5 after the decay ($\epsilon_{X_1} = \epsilon_{X_2} = 1/2$). One finds a dip around $k \simeq k_{\text{PT}}$ due to the anisotropic stress caused by X , as in Sec. 3, instead of a hill seen in the previous cases. In the low frequency limit $k \lesssim 10^{-2}k_{\text{PT}}$, the suppression by the anisotropic stress is less efficient because X_1 does not exist when such modes enter the horizon.

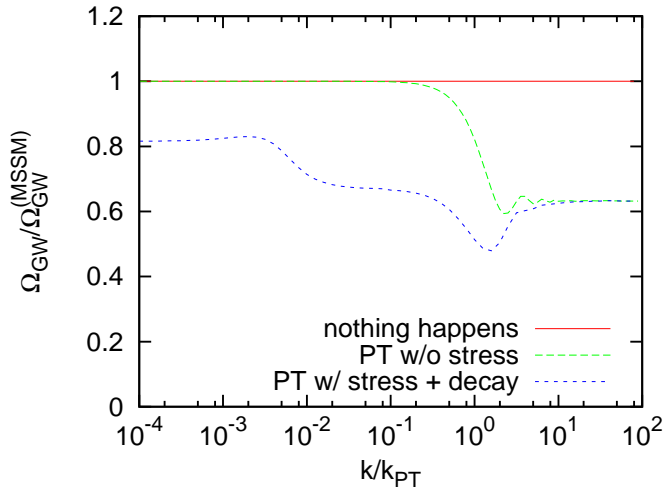


Figure 12: (Blue-dotted) GW spectrum for Case 3; the case with a short period of inflation, phase transition, instant decay into dark radiation and the decay of the dark radiation. ΔN_{eff} is assumed to be 1.3 at the decoupling and then decrease to 0.5 after the decay. (Red-solid) Flat GW spectrum expected in a simple RD universe. (Green-dashed) GW spectrum for the case without dark radiation.

4.4 Case 4

Let us consider the following cosmological scenario with late-time entropy production. The first two are the same as the Case 3.

1. A brief period of thermal inflation is caused by a scalar field ϕ .
2. After the phase transition, ϕ instantaneously decays into dark radiation X .
3. Non-relativistic matter dominates the universe.
4. Non-relativistic matter decays into radiation.

Non-relativistic matter exists in many models of phase transition since the coherent oscillation of the scalar field often survives after the phase transition. In this case, we use the following set of evolution equations:

$$\rho_{\text{vac}} = \begin{cases} \Lambda^4 & \text{for } t < t_{\text{PT}} \\ 0 & \text{for } t > t_{\text{PT}}, \end{cases} \quad (4.18)$$

$$\dot{\rho}_X + 4H\rho_X = \Lambda^4\delta(t - t_{\text{PT}}), \quad (4.19)$$

$$\dot{\rho}_m + 3H\rho_m = -\Gamma\rho_m, \quad (4.20)$$

$$\dot{\rho}_r + 4H\rho_r = \Gamma\rho_m, \quad (4.21)$$

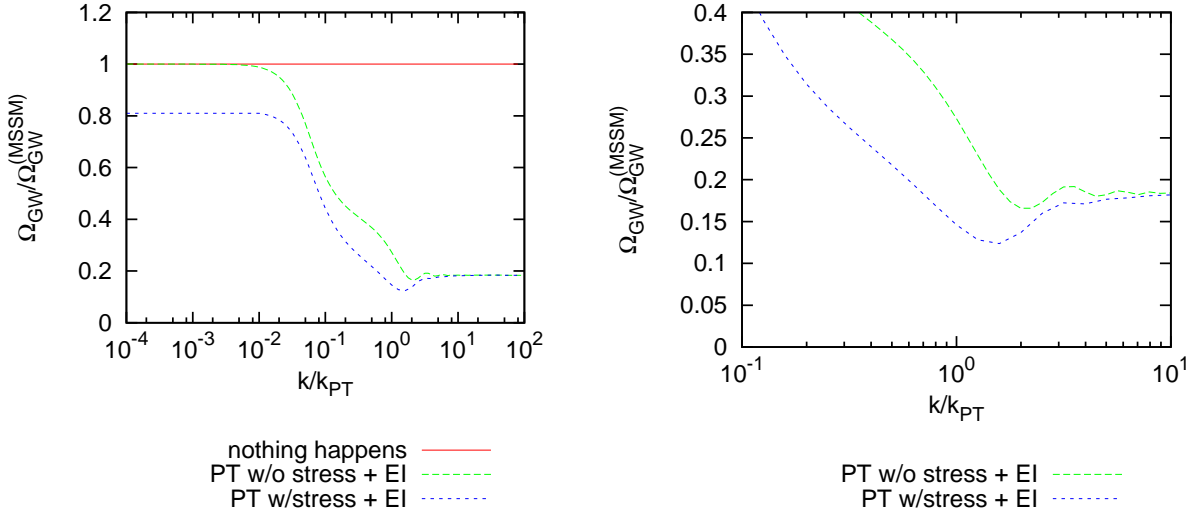


Figure 13: Left: (Blue-dotted) GW spectrum for Case 4. $R_{\text{coh}} = 0.1$, while $\Delta N_{\text{eff}} = 2$ and 0.5 just after the phase transition and after decay, respectively. (Red-solid) Flat spectrum expected in simple RD universe. (Green-dashed) GW spectrum for the case without dark radiation. Right: Blow-up of the left.

where $t_{\text{PT}} \ll \Gamma^{-1}$.

The resulting GW spectra are shown in Fig. 13 and Fig. 14. In these figures, we have varied the parameters R_{rad} and R_{coh} , which are defined as

$$R_{\text{rad}} \equiv \frac{\rho_{\text{rad}}}{\rho_{\text{tot}}} \Big|_{\text{just before PT}} = \frac{\rho_{\text{rad}}}{\rho_{\text{rad}} + \rho_{\text{vac}}} \Big|_{\text{just before PT}}, \quad (4.22)$$

and

$$R_{\text{coh}} \equiv \frac{\rho_{\text{coh}}}{\rho_{\text{vac}}} \Big|_{\text{just after PT}}, \quad (4.23)$$

with ρ_{coh} and ρ_{tot} being the energy density of the coherent oscillation and the total energy density, respectively. For the analysis of Case 4, we take $\rho_{\text{m}} = \rho_{\text{coh}}$. We have taken $R_{\text{coh}} = 0.1$ in Fig. 13, and $R_{\text{coh}} = 0.01$ in Fig. 14. The value of R_{rad} is chosen so that, with the assumption that the vacuum energy goes only into the coherent oscillation and dark radiation, the effective neutrino number ΔN_{eff} at the phase transition and subsequent reheating era is 2. In each case ΔN_{eff} is diluted to 0.5 after the entropy production. Note that the features of phase transition with anisotropic stress and entropy injection appear in the figure.

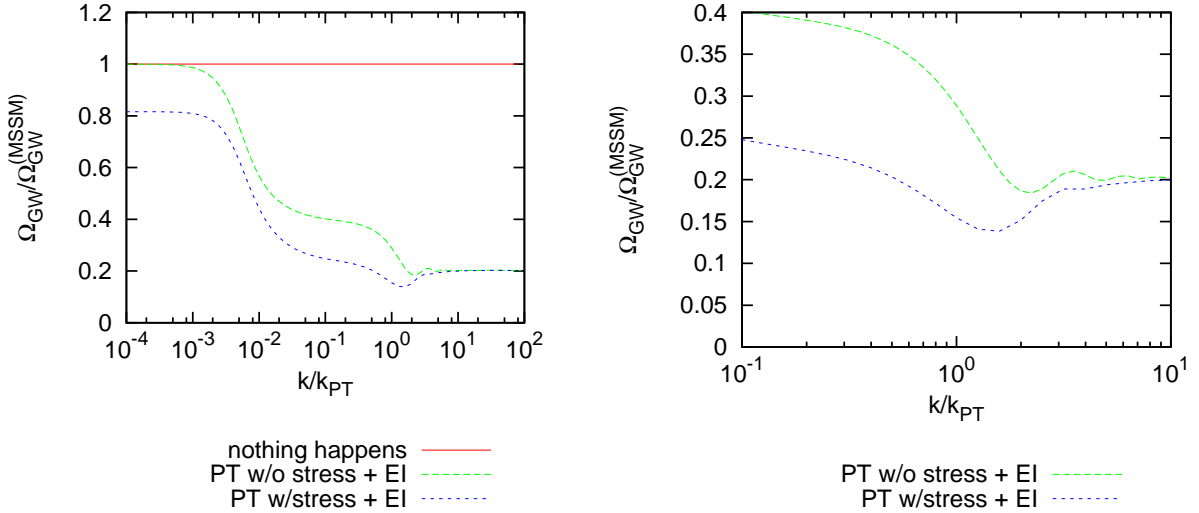


Figure 14: Left: GW spectrum for Case 4. $R_{\text{coh}} = 0.01$ and $\Delta N_{\text{eff}} = 2$ just after the phase transition is assumed. Right: Blow-up of the left.

4.5 Case 5

In the final example, the scalar field ϕ remains as a coherent oscillation after the phase transition. Thus we assume the following thermal history:

1. A brief period of thermal inflation is caused by a scalar field ϕ .
2. After the phase transition, ϕ begins a coherent oscillation, which behaves as non-relativistic matter.
3. The coherent oscillation ϕ decays into dark and visible radiation.

Then, the relevant evolution equations are:

$$\rho_{\text{vac}} = \begin{cases} \Lambda^4 & \text{for } t < t_{\text{PT}} \\ 0 & \text{for } t > t_{\text{PT}}, \end{cases} \quad (4.24)$$

$$\dot{\rho}_{\text{m}} + 3H\rho_{\text{m}} = -\Gamma\rho_{\text{m}} + \Lambda^4\delta(t - t_{\text{PT}}), \quad (4.25)$$

$$\dot{\rho}_{\text{r}} + 4H\rho_{\text{r}} = \Gamma B_{\text{r}}\rho_{\text{m}}, \quad (4.26)$$

$$\dot{\rho}_{\text{X}} + 4H\rho_{\text{X}} = \Gamma B_{\text{X}}\rho_{\text{m}}, \quad (4.27)$$

where B_{r} and B_{X} are branching ratio of ϕ into the radiation and dark radiation, respectively. They satisfy $B_{\text{r}} + B_{\text{X}} = 1$.

In Fig. 15 and Fig. 16, we show the resulting GW spectrum. In Fig. 15 we assumed a rather long period of thermal inflation and coherent oscillation domination. In the figure, the parameters are

$$\begin{aligned}
R_{\text{coh}} &= 1, \\
R_{\text{rad}} &= \frac{\rho_{\text{r}}}{\rho_{\text{tot}}}\Big|_{\text{just before PT}} = 10^{-6}, \\
R_{\text{dil}} &= \frac{a^4 \rho_{\text{tot}}\Big|_{\text{just after PT}}}{a^4 \rho_{\text{tot}}\Big|_{\text{well after decay}}} = 10^{-6},
\end{aligned}$$

and $B_X = 0$.

We can see that the GW spectrum scales as k^{-2} if the horizon entry is during the coherent-oscillation dominated era. For the modes which experience the horizon entry twice due to the thermal inflation, the GW spectrum shows oscillatory behavior with its amplitude proportional to k^{-4} . (See Appendix B.) We define k_{d} as the transition frequency between these two regimes. Note that R_{rad} parameterizes how much the initial radiation has been diluted by the short inflation, and therefore determines the ratio of the GW spectrum at $k \gg k_{\text{PT}}$ to that at $k = k_{\text{d}}$. On the other hand, R_{dil} gives how much the radiation which exists at the phase transition has been diluted by the subsequent matter domination, and determines the ratio of the GW spectrum at $k = k_{\text{d}}$ to at $k \ll k_{\text{decay}} \equiv aH(t = \Gamma^{-1})$.

Fig. 16, on the other hand, shows the GW spectrum with a short period of thermal inflation and coherent oscillation domination. Three lines (red-solid, green-dashed and blue-dotted) correspond to the parameters

$$\begin{aligned}
R_{\text{coh}} &= 1, \\
R_{\text{rad}} &= 0.67, 0.5, 0.33, \\
R_{\text{dil}} &= 0.5,
\end{aligned}$$

and we have taken B_X so that we obtain $\Delta N_{\text{eff}} = 0$ (0.5) at present in the left (right) figure. Although the spectral shapes for the cases with and without dark radiation look similar, the detailed structures are different. Thus, precise observations of the height of the spectrum at $k \ll k_{\text{PT}}$ and the amplitude of the oscillation around $k \simeq (\text{a few}) \times k_{\text{PT}}$ may make it possible to tell the existence of the anisotropic stress.

5 Model

In this section we show that some particle-physics-motivated models can realize the Cases 1–5 discussed in the previous section. We take up two models for example, a SUSY PQ model and a SUSY majoron model.

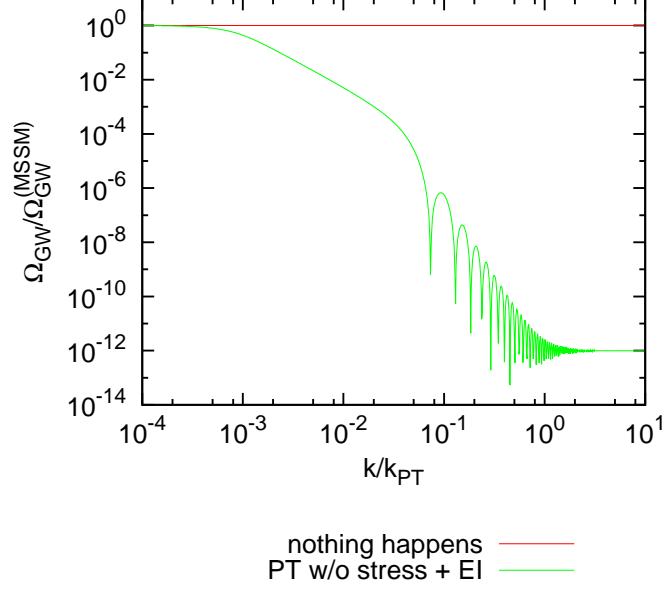


Figure 15: GW spectrum for Case 5, taking $R_{\text{coh}} = 1$, $R_{\text{rad}} = 10^{-6}$ and $R_{\text{dil}} = 10^{-6}$.

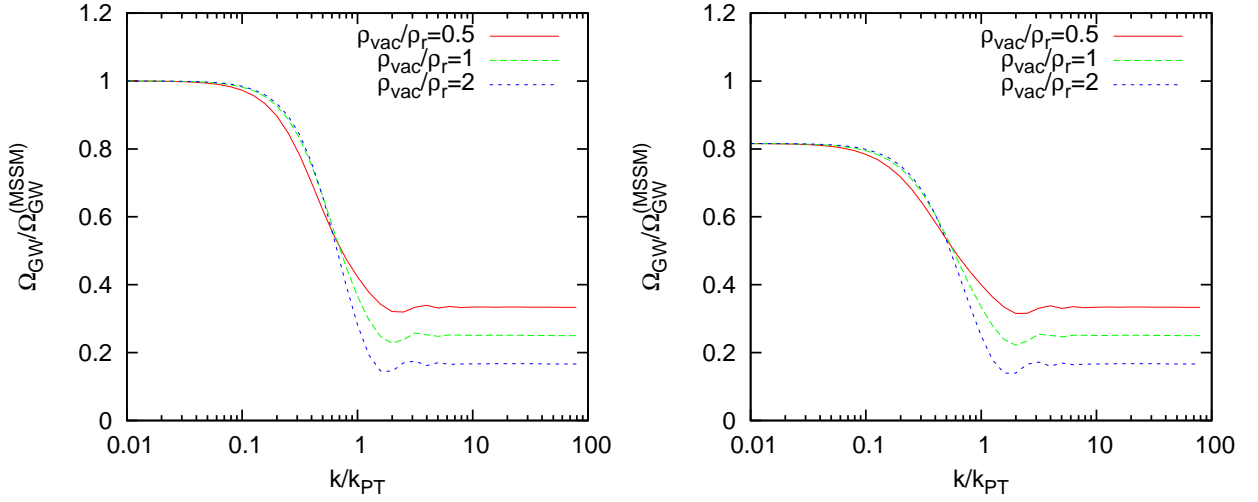


Figure 16: Left: GW spectrum for Case 5 for $R_{\text{coh}} = 1$, $R_{\text{dil}} = 0.5$ and $R_{\text{rad}} = 0.67, 0.5, 0.33$ for the red-solid, green-dashed, blue dotted lines, respectively. We also assumed $\Delta N_{\text{eff}} = 0$. Right: Same as left but for $\Delta N_{\text{eff}} = 0.5$.

5.1 SUSY Peccei-Quinn model

We consider a SUSY PQ model [28]. In particular, we consider the model with the following superpotential:

$$W = \lambda S(\Phi\bar{\Phi} - f^2) + y_1\Phi Q_i\bar{Q}_i + y_2\bar{\Phi}Q'_j\bar{Q}'_j, \quad (5.1)$$

where Q, Q' and \bar{Q}, \bar{Q}' are PQ quarks which are in the fundamental and anti-fundamental representations of color $SU(3)$, respectively, and f is the PQ scale. The superpotential has a PQ symmetry: $\Phi \rightarrow \Phi e^{i\alpha}$, $\bar{\Phi} \rightarrow \bar{\Phi} e^{-i\alpha}$, $Q \rightarrow Q e^{-i\alpha}$ and $Q' \rightarrow Q' e^{i\alpha}$. The indices i and j run from 1 to a_1 and a_2 , respectively.^{#7} In order for the PQ symmetry to be anomalous under the color $SU(3)$ for solving the strong CP problem, we need $a_1 \neq a_2$. For simplicity, we assume that the Yukawa couplings y_1 and y_2 are independent of the indices i and j . The soft SUSY breaking potential is given by

$$V_{\text{soft}} = m^2 |\Phi|^2 + m^2 |\bar{\Phi}|^2 + m^2 |S|^2. \quad (5.2)$$

Here we have assumed that the soft masses m are the same for $\Phi, \bar{\Phi}$ and S for simplicity and neglected trilinear terms.^{#8} We rewrite the two superfields Φ and $\bar{\Phi}$ in terms of the axion multiplet A and heavy multiplet A_H as

$$\Phi = \langle \Phi \rangle + A \cos \theta + A_H \sin \theta, \quad (5.3)$$

$$\bar{\Phi} = \langle \bar{\Phi} \rangle - A \sin \theta + A_H \cos \theta, \quad (5.4)$$

where $\tan \theta = \langle \bar{\Phi} \rangle / \langle \Phi \rangle$. The axion a and saxion σ are embedded in the scalar component of A as $A = (\sigma + ia)/\sqrt{2}$. As long as the SUSY breaking mass is much smaller than the PQ scale, Φ and $\bar{\Phi}$ are constrained on $\Phi\bar{\Phi} = f^2$.

For sufficiently high cosmic temperature, the thermal effects keep Φ and $\bar{\Phi}$ at the origin. As the temperature decreases, Φ and $\bar{\Phi}$ begin to roll down toward the minimum. The mass matrix for Φ and $\bar{\Phi}$ around the origin, including thermal effects, is given by

$$M^2 \sim \begin{pmatrix} y^2 T^2 & -\lambda^2 f^2 \\ -\lambda^2 f^2 & y^2 T^2 \end{pmatrix}, \quad (5.5)$$

where $y \sim \sqrt{a_1} y_1 \sim \sqrt{a_2} y_2$. Note that, if a_1 and a_2 are larger than 1, $y \gtrsim 1$ is possible even if $y_1, y_2 \lesssim 1$. Thus the temperature at the time of phase transition is evaluated as

$$T_{\text{PT}} \sim \frac{\lambda}{y} f, \quad (5.6)$$

where, in our analysis, we assume that $y \gtrsim \lambda$. The ratio of radiation energy density to the total one just before the phase transition is then given by

$$R_{\text{rad}} = \frac{\frac{\pi^2}{30} g_* T_{\text{PT}}^4}{\frac{\pi^2}{30} g_* T_{\text{PT}}^4 + \lambda^2 f^4}. \quad (5.7)$$

^{#7} In order to avoid the axionic domain wall problem, we need $|a_2 - a_1| = 1$ in the hadronic axion model [29].

^{#8} Giving different soft masses to each field may shift the potential minimum and change axion decay constant by some factor, but the following qualitative argument does not change.

If there is no production of dark radiation, the ratio R_{rad} also corresponds to the relative magnitude of the GW spectrum, $\Omega_{\text{GW}}(k \gg k_{\text{PT}})/\Omega_{\text{GW}}(k \ll k_{\text{PT}})$, as discussed in the previous sections.

After the phase transition, we only consider the effects of the particles in the axion multiplet A . Other particles in the PQ sector have masses larger than T_{PT} if $y \gtrsim 1$, which we will assume in this subsection. Then, we may eliminate $\bar{\Phi}$ in terms of Φ by using $\Phi\bar{\Phi} = f^2$, and obtain the potential for the scalar component of Φ . For the study of the behavior of the axion multiplet in the early universe, it is important to take account of various thermal effects [30, 31, 32]. In particular, the effective potential of Φ is given in the following form:

$$V = V_0 + V_L + V_T. \quad (5.8)$$

Here, V_0 is the soft-mass term

$$V_0 = m^2 |\Phi|^2 + m^2 |\bar{\Phi}|^2 = m^2 |\Phi|^2 + m^2 \frac{f^4}{|\Phi|^2}. \quad (5.9)$$

In addition, V_L and V_T represent thermal effects. V_L is the thermal log potential [33], which comes from the fact that the masses of PQ quarks depend on the amplitude of Φ :

$$V_L \simeq - \sum_{\text{heavy quarks } Q} \alpha_L \alpha_3^2 T^4 \ln |m_Q^2(\Phi)| \simeq -2(a_2 - a_1) \alpha_3^2 T^4 \ln |\Phi|. \quad (5.10)$$

Note that V_L is effective when the temperature is lower than the masses of PQ quarks. Furthermore, V_T is the thermal potential

$$V_T = \begin{cases} \frac{1}{24} T^2 m_{\bar{Q}}(\Phi)^2 & (\text{for 1 real scalar}) \\ \frac{1}{24} T^2 m_Q(\Phi)^2 & (\text{for 1 Weyl fermion}) \end{cases}, \quad (5.11)$$

where $m_{\bar{Q}}(\Phi)$ and $m_Q(\Phi)$ are masses of PQ squarks and PQ quarks, respectively. Note that V_T is effective when the PQ quarks are in the thermal bath, in contrast to V_L . The minimum of the potential depends on the temperature. First, in the low-temperature limit, $|\Phi|_{\text{min}} \sim f$. If the thermal log potential is efficient, the minimum is given by $|\Phi|_{\text{min}} \sim \alpha_3 T^2/m$. Finally, in the high-temperature limit, the thermal mass term determines the minimum at $|\Phi|_{\text{min}} \sim (yTf^2/m)^{1/2}$.

The trajectory of the PQ fields (in particular, Φ and $\bar{\Phi}$) during the phase transition depends on a_i and y_i . Therefore it may be the case that a considerable fraction of the initial vacuum energy may be transferred to the energy density of the saxion coherent oscillation. By using the parameter R_{coh} given in Eq. (4.23), we phenomenologically parameterize the fraction of ρ_{vac} transferred into the coherent oscillation energy density ρ_{coh} ; the fraction $1 - R_{\text{coh}}$ of ρ_{vac} , which corresponds to the energy density of the oscillation of the field

transverse to the trajectory $\Phi\bar{\Phi} = f^2$, is assumed to be instantly transferred into the energy densities of the axion and saxion:

$$\rho_a \sim \rho_\sigma \sim \frac{1 - R_{\text{coh}}}{2} \rho_{\text{vac}}. \quad (5.12)$$

Hereafter we consider the case where the initial vacuum energy does not go into the visible radiation. If R_{coh} is not negligible, the amplitudes of Φ or $\bar{\Phi}$ can take large value due to the dynamics along the saxion direction. The maximal value of $|\Phi|$ during the coherent oscillation is

$$|\Phi|_{\text{max}} \simeq \frac{\lambda f^2 R_{\text{coh}}^{1/2}}{m}. \quad (5.13)$$

Using $m_{Q'} = yf^2/|\Phi|$ and $T_{\text{PT}} \sim \lambda f/y$, the PQ quarks are not in thermal equilibrium if

$$\left(\frac{y}{\lambda}\right)^2 > \frac{f}{m}. \quad (5.14)$$

If this condition is satisfied, the saxion may be trapped at the local minimum and the onset of the saxion coherent oscillation may be delayed.

The subsequent evolution of the system depends on the decay rate and dissipation rate of the fields. First, let us consider the collision rate of the particles in the PQ sector. Without PQ quarks in the thermal bath, the axion, saxion, and axino hardly communicate with the visible sector particles. Then, they may be sequestered from the visible sector and the temperature of the PQ-sector particles may be different from that of the visible-sector particles. In particular, if the temperature of the PQ sector particles, denoted as $T^{(\text{PQ})}$, is lower than $\sim \lambda f$, the collision rate among the PQ sector particles is approximately given by

$$\Gamma_{\text{coll}} \simeq 4 \times 10^{-4} \frac{T^{(\text{PQ})5}}{f^4}. \quad (5.15)$$

Thus, when $T^{(\text{PQ})}$ becomes lower than the decoupling temperature $T_{\text{decouple}}^{(\text{PQ})}$, the PQ-sector particles behave as dark radiation (as long as they are relativistic), where $T_{\text{decouple}}^{(\text{PQ})}$ is estimated as

$$T_{\text{decouple}}^{(\text{PQ})} \sim 2 \times 10^{11} \text{ GeV} \times \left(\frac{f}{10^{12} \text{ GeV}}\right)^{4/3}. \quad (5.16)$$

Here the ratio of the energy density of the visible sector to the invisible one is $R_{\text{rad}}/(1 - R_{\text{rad}})$ in the absence of the saxion coherent oscillation, therefore the temperature of the visible sector at the time of the decoupling of the PQ-sector particles is

$$T_{\text{decouple}} = 0.36 \times \left(\frac{R_{\text{rad}}}{1 - R_{\text{rad}}}\right)^{1/4} T_{\text{decouple}}^{(\text{PQ})}. \quad (5.17)$$

We also comment here that the effect of dissipation may be important in studying the evolution of the saxion in thermal bath [31]. When PQ quarks are not in thermal equilibrium ($m_Q \gtrsim T$), the dissipation rate of the axion, saxion and axino via the scattering with the gluon is [34]

$$\Gamma_{\text{diss}} \sim \frac{9\alpha_3^2}{128\pi^2 \ln \alpha_3^{-1}} \frac{T^3}{\max(\Phi, \bar{\Phi})^2}. \quad (5.18)$$

When PQ quarks are in thermal bath, on the other hand, (s)axions collide with particles in the heavier multiplets with the rate

$$\Gamma_{\text{diss}} \sim 10^{-2} \times y^4 T. \quad (5.19)$$

With the choices of parameters for the following discussion, however, Γ_{diss} is smaller than the expansion rate of the universe so that the effects of dissipation are irrelevant. It means that the scattering rate between the PQ sector and visible sector is so small that the PQ sector is sequestered from the visible sector. Thus we can define the temperature of the PQ sector and the visible sector separately.

After the decoupling, the saxion decays at the late epoch. The partial decay rates of the saxion into axion and gluon pairs are

$$\Gamma_{\sigma \rightarrow aa} \simeq \frac{1}{64\pi} \frac{m^3}{f^2}, \quad (5.20)$$

$$\Gamma_{\sigma \rightarrow gg} \simeq \frac{\alpha_3^2}{32\pi^3} \frac{m^3}{f^2}, \quad (5.21)$$

respectively, where, in deriving Eq. (5.20), we assumed that the difference of the vacuum expectation values of Φ and $\bar{\Phi}$ is sizable. In addition, if Φ couples to the Higgs doublets, as $\Phi H_u H_d$, for example, and also if the higgsino mass is dominantly from the vacuum expectation value of Φ , the saxion may also decay into the Higgs-boson pair with the following decay rate:

$$\Gamma_{\sigma \rightarrow HH} \simeq \frac{1}{2\pi} \frac{m^3}{f^2} \left(\frac{\mu}{m} \right)^4, \quad (5.22)$$

where μ is the higgsino mass. The decay temperature of the saxion is estimated by solving the following equation:

$$\frac{m}{\langle E_\sigma \rangle(T_{\text{decay}})} \Gamma_\sigma \sim 3H(T_{\text{decay}}), \quad (5.23)$$

where $\langle E_\sigma \rangle(T)$ is the averaged energy of saxion at the cosmic temperature T . The decay temperature depends on the dominant decay mode of the saxion, and also on the typical energy of the saxion at the time of the decay. If $R_{\text{coh}} \sim 0$ and $R_{\text{rad}} \sim 0$ and the saxion

dominantly decays into the Higgs pair, the temperature of the visible sector T_{decay} just after the decay is estimated as

$$T_{\text{decay}} \sim 4 \times 10^3 \text{ GeV} \times \left(\frac{\mu}{10^5 \text{ GeV}} \right)^{4/3} \left(\frac{f}{10^{12} \text{ GeV}} \right)^{-2/3}. \quad (5.24)$$

where we approximated that $\langle E_\sigma \rangle \sim T^{(\text{PQ})}$ and used $g_*^{(\text{PQ})} = 3.75$ as the effective number of relativistic degrees of freedom in the PQ sector, and also assumed that the saxion decays while being relativistic. If the saxion decays after becoming non-relativistic, we obtain

$$T_{\text{decay}} \sim 5 \times 10^3 \text{ GeV} \times \left(\frac{\mu}{10^5 \text{ GeV}} \right)^2 \left(\frac{m}{10^5 \text{ GeV}} \right)^{-1/2} \left(\frac{f}{10^{12} \text{ GeV}} \right)^{-1}. \quad (5.25)$$

Now let us see that the SUSY axion model can realize the Cases 1 and 2 studied in Sec. 4.1 and Sec. 4.2, respectively. The role of ϕ is played by the PQ scalar, Φ and $\bar{\Phi}$. After the PQ phase transition, they decay into particles in the axion multiplet, which are thermalized due to their self interactions. (Here, we assume that the thermal bath of the PQ sector particles are sequestered from that of the visible sector.) At some point, the interactions of the PQ sector particles become very weak. Then, the mean free path of the axion and saxion becomes so long that they behave as dark radiation X . After some periods, the saxion decays into radiation. If the saxion decays while it is relativistic, it corresponds to the Case 1 and if it is non-relativistic, the Case 2 is realized.

A sample parameter set corresponding to the Case 1 is

$$\begin{aligned} f &= 10^{12} \text{ GeV}, \\ \mu &= m = 10^6 \text{ GeV}, \\ \lambda &= 1, \\ y &= 2, \\ R_{\text{coh}} &= 0. \end{aligned} \quad (5.26)$$

With the above parameters, we obtain

$$\begin{aligned} T_{\text{PT}} &\simeq 10^{12} \text{ GeV}, \\ T_{\text{decouple}} &\simeq 10^{11} \text{ GeV}, \\ T_{\text{decay}} &\simeq 10^6 \text{ GeV}, \\ R_{\text{rad}} &\simeq 0.8. \end{aligned} \quad (5.27)$$

The cosmological evolution goes as follows.

- After the phase transition, the radial oscillation of Φ and $\bar{\Phi}$ quickly decays into the particles in the axion multiplet.
- After the temperature drops down to $T \simeq T_{\text{decouple}}$, the collision rate in the PQ sector becomes smaller than the Hubble expansion rate. So axion, saxion and axino freely stream and hence behave as dark radiation.

- If the field Φ or $\bar{\Phi}$ couples to the Higgs sector, the saxion can mainly decays into the Higgs bosons. The saxion decays at $T = T_{\text{dec}} \simeq 10^6$ GeV before it becomes massive. This eliminates about one-third of dark radiation. If the axino also decays without dominating the universe, $\Delta N_{\text{eff}} \sim 1$ at the present universe.

The features of the GW spectrum expected with the above setup are the same as Fig. 9, but the positions of the characteristic wavenumber are different. In Fig. 9, $T_{\text{decouple}} = 10^{-2}T_{\text{PT}}$ and $T_{\text{decay}} = 10^{-4}T_{\text{PT}}$ is assumed while in the present setup they become $T_{\text{decouple}} = 10^{-1}T_{\text{PT}}$ and $T_{\text{decay}} = 10^{-6}T_{\text{PT}}$.

A sample parameter set corresponding to the Case 2 is,

$$\begin{aligned}
f &= 10^{12} \text{ GeV}, \\
\mu &= m = 10^5 \text{ GeV}, \\
\lambda &= 1, \\
y &= 2, \\
R_{\text{coh}} &= 0,
\end{aligned} \tag{5.28}$$

which gives

$$\begin{aligned}
T_{\text{PT}} &\simeq 10^{12} \text{ GeV}, \\
T_{\text{decouple}} &\simeq 10^{11} \text{ GeV}, \\
T_{\text{decay}} &\simeq 10^4 \text{ GeV}, \\
R_{\text{rad}} &= 0.8.
\end{aligned} \tag{5.29}$$

The cosmological evolution goes as follows.

- After the phase transition, the radial oscillation of Φ and $\bar{\Phi}$ quickly decays into the PQ sector.
- After the temperature drops down to $T \simeq T_{\text{decouple}}$, the collision rate in the PQ sector becomes smaller than the Hubble expansion rate, and the axion, saxion and axino become dark radiation.
- The saxion becomes non-relativistic at $T \simeq m = 10^5$ GeV. Then, it decays into the Higgs bosons at $T_{\text{dec}} \simeq 10^4$ GeV.

The features in the GW spectrum with this setup are expected to be the same as in Fig. 10 and Fig. 11, although the characteristic wavenumbers are different.

If a large amount of the vacuum energy once goes into the coherent oscillation of the saxion, the Case 5 may also be realized in the SUSY PQ model. With a proper choice of parameters, most of the vacuum energy goes to the coherent oscillation of the saxion. The saxion dominates the universe and then decays; significant amount of the axion, which plays the role of dark radiation, may be produced by the decay with a relevant choice of parameters.

In this setup, the initial radiation is first diluted by the vacuum energy just like in the previous cases, and then diluted by the matter (i.e., saxion) domination which begins just after the phase transition. The former dilution can be parameterized by R_{rad} previously defined. Let us define the quantity R_{dil} , which parameterize the latter dilution:

$$R_{\text{dil}} \equiv \frac{a^4 \rho_{\text{tot}}|_{\text{just after PT}}}{a^4 \rho_{\text{tot}}|_{\text{well after decay}}} \simeq 2 \times 10^{-11} \lambda^{-4/3} y^{4/3} \left(\frac{\mu}{10^5 \text{ GeV}} \right)^{8/3} \left(\frac{m}{10^5 \text{ GeV}} \right)^{-2/3} \left(\frac{f}{10^{12} \text{ GeV}} \right)^{-8/3}. \quad (5.30)$$

This determines the ratio of the spectral height at $k = k_d$ to that at $k \ll k_{\text{decay}} \equiv aH(t = \Gamma^{-1})$.

The first example in the Case 5 discussed in Sec. 4.5 is realized with the following parameters:

$$\begin{aligned} f &= (\text{a few}) \times 10^{11} \text{ GeV}, \\ \mu &= m = 10^6 \text{ GeV}, \\ \lambda &= 10^{-3}, \\ y &= 1, \\ R_{\text{coh}} &= 1, \end{aligned} \quad (5.31)$$

which result in

$$\begin{aligned} T_{\text{PT}} &\simeq 10^8 \text{ GeV}, \\ R_{\text{rad}} &\simeq 10^{-4}, \\ R_{\text{dil}} &\simeq 10^{-4}. \end{aligned} \quad (5.32)$$

Thus, the cosmological evolution goes as follows:

- The thermal inflation caused by the vacuum energy of Φ and $\bar{\Phi}$ dilutes the initial visible radiation by a factor of 10^{-4} .
- After the phase transition, almost all the vacuum energy goes to the saxion coherent oscillation. The heavy quarks remain massive since Eq. (5.14) is satisfied.
- After the coherent oscillation dilutes the radiation further by a factor of 10^{-4} , it decays into visible radiation.

The second example in the Case 5 is realized with the following parameters:

$$\begin{aligned} f &= (\text{a few}) \times 10^9 \text{ GeV}, \\ \mu &= m = 10^6 \text{ GeV}, \\ \lambda &= 10^{-1}, \\ y &= 1, \\ R_{\text{coh}} &= 1, \end{aligned} \quad (5.33)$$

which give

$$\begin{aligned} T_{\text{PT}} &\simeq 10^8 \text{ GeV}, \\ R_{\text{rad}} &= \mathcal{O}(0.1), \\ R_{\text{dil}} &= \mathcal{O}(0.1). \end{aligned}$$

The cosmological evolution goes as follows:

- The thermal inflation caused by the vacuum energy of Φ and $\bar{\Phi}$ dilutes the initial visible radiation by a factor of $\mathcal{O}(0.1)$.
- After the phase transition, almost all the vacuum energy goes to the saxion coherent oscillation. The heavy quarks remain massive since Eq. (5.14) is satisfied.
- The coherent oscillation dilutes the radiation by a factor of $\mathcal{O}(0.1)$, and it soon decays into visible radiation.

5.2 SUSY majoron model

Next, we consider a SUSY majoron model [35, 36]. The mass of the right-handed neutrino, which is needed for the seesaw mechanism [37], can be generated as a consequence of U(1) symmetry breaking. This U(1) may be identified as a gauged $B - L$ symmetry, or it can be global lepton number symmetry. Here we consider the latter option. Then a Nambu-Goldstone (NG) boson appears which is associated with the spontaneous breakdown of the U(1) global symmetry. This NG boson is called majoron. (We call other fields in the majoron supermultiplet as smajoron, which is a real scalar field, and majorino, which is the fermionic superpartner of the majoron.)

Let us consider the following superpotential as an example of a SUSY majoron model,

$$W = \lambda S(\Phi\bar{\Phi} - f^2) + y_i\Phi N_i N_i + y'_i\bar{\Phi} N'_i N'_i, \quad (5.34)$$

where N_i are the right-hand neutrinos, while Φ and $\bar{\Phi}$ are lepton-number violating fields. In the following argument, we take $y_i = y'_i = y$ for simplicity. In addition, we also introduce N'_i which have opposite lepton number. In contrast to the SUSY PQ model, this model does not lead to the thermalization of the majoron sector with the SM sector since the neutrino Yukawa coupling constants are taken to be small enough. Note also that the parameter f , the U(1) symmetry breaking scale, is not severely constrained in contrast to the PQ scale.

In the following, we assume that the majoron and the right-handed neutrinos are initially in the thermal bath. (We use the same notation as in the previous section for T_{PT} , T_{decouple} , T_{decay} , R_{coh} and R_{rad} .)

Now let us see that the SUSY majoron model can realize the Case 3 and 4 studied in Sec. 4.3 and Sec. 4.4. For the Case 3, we take the following parameters:

$$\begin{aligned}
f &= 10^{10} \text{ GeV}, \\
\mu &= m = (\text{a few}) \times 10^5 \text{ GeV}, \\
\lambda &= 10^{-3}, \\
y &= 10^{-1}, \\
R_{\text{coh}} &= 0.
\end{aligned} \tag{5.35}$$

Then, we obtain

$$\begin{aligned}
T_{\text{PT}} &\simeq 10^8 \text{ GeV}, \\
T_{\text{decay}} &\simeq 10^6 \text{ GeV}.
\end{aligned} \tag{5.36}$$

The cosmological evolution goes as follows:

- After the phase transition, the radial oscillation of Φ and $\bar{\Phi}$ quickly decays into the majoron sector. The majoron sector does not thermalize because of the weakness of the interaction of the majoron.
- The smajoron decays at $T = T_{\text{dec}} \simeq 10^6 \text{ GeV}$ before it becomes massive. This eliminates about one-half of the dark radiation, realizing the present $\Delta N_{\text{eff}} = \mathcal{O}(0.1)$.

For the Case 4, we take the following parameters:

$$\begin{aligned}
f &= 10^{11} \text{ GeV}, \\
\mu &= m = 10^6 \text{ GeV}, \\
\lambda &= 10^{-5}, \\
y &= 10^{-2}, \\
R_{\text{coh}} &= 0.01, 0.1.
\end{aligned} \tag{5.37}$$

The value of R_{coh} corresponds to Fig. 13 and Fig. 14, respectively. With the above choice of parameters,

$$\begin{aligned}
T_{\text{PT}} &\simeq 10^8 \text{ GeV}, \\
T_{\text{decay}} &\simeq 10^6 \text{ GeV}.
\end{aligned} \tag{5.38}$$

The cosmological evolution goes as follows:

- After the phase transition, a small fraction of the vacuum energy goes into the coherent oscillation of the smajoron. The rest, the radial oscillation of Φ and $\bar{\Phi}$, quickly decays into the majoron sector particles. The majoron sector does not thermalize.

- The coherent oscillation of the smajoron begins to dominate the universe after the temperature decreases to $10^{-1}T_{\text{PT}}$ and $10^{-2}T_{\text{PT}}$ in Fig. 13 and Fig. 14, respectively. This dilutes the dark radiation produced at the phase transition. Note that the smajoron particles are still relativistic or just becoming non-relativistic at these temperatures.
- The coherent oscillation (and smajoron particles in the case of Fig. 14,) decays into visible radiation and the present ΔN_{eff} becomes $\mathcal{O}(0.1)$.

6 Conclusions

In this paper we have studied various effects of the cosmological events in the early universe on the inflationary GW spectrum. In particular, some (well-motivated) models of cosmological phase transition, including the PQ phase transition, in general lead to complicated structures in the GW spectrum, which might be detectable in future space-based GW detectors [15, 16, 17]. Hence, if the spectrum of the inflationary GWs is determined by future experiments, it will give clues to the high-energy physics beyond the reach of accelerator experiments.

Finally we mention inflation models which predict observable levels of GWs. Although the recent Planck results do not favor the standard chaotic inflation model with a simple power-law potential [39], a class of large field models has been proposed which fits the Planck results well while predicts the tensor-to-scalar ratio of $r \sim \mathcal{O}(0.01)$ [40, 41] (see Refs. [42] for early attempts). The Higgs inflation [43, 44, 45] predicts $r \sim \mathcal{O}(10^{-3})$, which is within the reach of future GW detectors.^{#9} The R^2 -inflation model [49] (see Refs. [50, 51] for its generalization) and topological inflation [52, 53, 54] also predict observable GWs with $r \sim \mathcal{O}(10^{-3})$.

Acknowledgment

We thank K. Schmitz for comments regarding footnote #3. This work is supported by Grant-in-Aid for Scientific research from the Ministry of Education, Science, Sports, and Culture (MEXT), Japan, No. 22244021 (T.M.), No. 22540263 (T.M.), No. 23104001 (T.M.), No. 21111006 (K.N.), and No. 22244030 (K.N.). The work of R.J. is supported in part by JSPS Research Fellowships for Young Scientists.

A Inflationary GW power spectrum

The dimensionless power spectrum $\Delta^2(k)$ of some perturbation $\delta(\mathbf{x})$ which obeys a homogeneous and isotropic distribution is defined as

$$\langle \delta(\mathbf{x})\delta(\mathbf{x}') \rangle = \int \frac{d^3k}{(2\pi)^3} e^{i\mathbf{k}\cdot\mathbf{x}} P_\delta(k) = \int \frac{dk}{k} \Delta^2(k) \frac{\sin(kr)}{kr}, \quad (\text{A.1})$$

^{#9} For other types of Higgs inflation, see Refs. [46, 47, 48].

where $r = |\mathbf{x} - \mathbf{x}'|$ and the bracket means taking ensemble average, which we assume to be the same as spacial average. In terms of Fourier-transformed perturbation $\delta(\mathbf{k})$, $\Delta(k)$ is written as

$$\Delta^2(k) = \frac{k^3}{2\pi^2} P_\delta(k), \quad (\text{A.2})$$

where

$$\langle \delta(\mathbf{k}) \delta(\mathbf{k}') \rangle \equiv (2\pi)^3 \delta(\mathbf{k} + \mathbf{k}') P_\delta(k). \quad (\text{A.3})$$

In the present case $\delta(\mathbf{x})$ corresponds to $h_{ij}(t, \mathbf{x})$:

$$\Delta_{\text{GW}}^2(t, k) = \frac{k^3}{2\pi^2} P_h(t, k), \quad (\text{A.4})$$

where

$$\sum_{\lambda=+, \times} \langle h(t, \mathbf{k}, \lambda) h(t, \mathbf{k}', \lambda) \rangle \equiv (2\pi)^3 \delta(\mathbf{k} + \mathbf{k}') P_h(t, k). \quad (\text{A.5})$$

In the inflationary era the perturbations with wavenumbers of our interest go far out of the horizon because of the exponential growth of the scale factor. Since then $h(t, \mathbf{k}, \lambda)$ is constant until it re-enters the horizon, and hence $\Delta_{\text{GW}}^2(t, k)$ is constant in time outside the horizon:

$$\Delta_{\text{GW}}^2(t, k) = \Delta_{\text{GW,prim}}^2(k) \quad \text{for } k \ll aH. \quad (\text{A.6})$$

Here ‘‘prim’’ means its primordial value, evaluated at the time after the horizon exit. On the other hand, as shown in Sec. 2, the amplitude of GWs decreases as a^{-1} inside the horizon ($k \gg aH$). Hence,

$$\langle \Delta_{\text{GW}}^2(t, k) \rangle_{\text{osc}} = \frac{1}{2} \Delta_{\text{GW,prim}}^2(k) \left(\frac{a_{\text{hi}}(k)}{a(t)} \right)^2 \quad \text{for } k \gg aH, \quad (\text{A.7})$$

where $\langle \dots \rangle_{\text{osc}}$ is for oscillation average. Here, $a_{\text{hi}}(k)$ is the scale factor at which the mode k enters the horizon $k/H = a_{\text{hi}}(k)$. Note the factor 1/2 here is from the fact that h is oscillating with high frequency inside the horizon.^{#10}

Assuming a slow-roll inflation and the canonical commutation relation of h_{ij} , one obtains [38]

$$\Delta_{\text{GW,prim}}^2(k) = 64\pi G \left(\frac{H_{\text{ho}}(k)}{2\pi} \right)^2, \quad (\text{A.8})$$

^{#10} Here we have considered GWs entering the horizon at the RD era. For those entering in the MD era, the factor 1/2 in Eq. (A.7) should be replaced with 9/32, which is derived from the analytical solution given in Eq. (2.11).

where H_{ho} is the value of H at the time of horizon exit $k = aH$. Because GWs of different wavenumbers exit the horizon at different epochs, H_{ho} depends on k :

$$H_{\text{ho}}^2(k) = H_{\text{ho}}^2(k_0) \left(\frac{k}{k_0} \right)^{n_t}, \quad (\text{A.9})$$

where $k_0 = 0.002 \text{Mpc}^{-1}$ is the pivot scale and n_t is the tensor spectral index.

Now, we relate the energy density of inflationary GWs to Δ_{GW}^2 . We define the effective energy-momentum tensor of GWs as

$$T_{\mu\nu}^{\text{GW}}(t, \mathbf{x}) = -\frac{1}{32\pi G} \langle h^{ij}{}_{;\mu} h_{ij;\nu} \rangle_{\text{osc}}(t, \mathbf{x}), \quad (\text{A.10})$$

where $\langle \dots \rangle_{\text{osc}}$ here indicates the oscillation average as well as the ensemble average; note that this expression is applicable only to GWs with subhorizon modes $k \gg aH$. The effective energy density of GWs is then defined as

$$\rho_{\text{GW}}(t, \mathbf{x}) \equiv [T_{\text{GW}}]{}^0{}_0(t, \mathbf{x}) = \frac{1}{32\pi G} \langle h^{ij;0} h_{ij;0} \rangle_{\text{osc}}(t, \mathbf{x}). \quad (\text{A.11})$$

We define the effective energy of GWs per logarithmic frequency $\rho_{\text{GW}}(t, k)$ through

$$\rho_{\text{GW}}(t) \equiv \int d \ln k \rho_{\text{GW}}(t, k), \quad (\text{A.12})$$

where we have assumed the homogeneity and isotropy of the primordial GWs. Because of the subhorizon condition $k \gg aH$, we may neglect terms with time derivative on the scale factor in Eq. (A.11). If the universe is filled with perfect fluid at t , Eq. (2.7) tells us that h is a harmonic oscillator with frequency k/a . Thus for subhorizon modes, we can use the relation $\langle \dot{h}_{ij}^2 \rangle_{\text{osc}} = \langle (k/a)^2 h_{ij}^2 \rangle_{\text{osc}}$ to write $\rho_{\text{GW}}(t, k)$ as

$$\rho_{\text{GW}}(t, k) = \frac{1}{32\pi G} \frac{k^2}{a^2} \frac{k^3}{2\pi^2} P_h(t, k) = \frac{1}{32\pi G} \frac{k^2}{a^2} \Delta_{\text{GW}}^2(t, k). \quad (\text{A.13})$$

The GW spectrum $\Omega_{\text{GW}}(t, k)$ is defined as the fraction of $\rho_{\text{GW}}(t, k)$ to the critical density:

$$\Omega_{\text{GW}}(t, k) \equiv \frac{\rho_{\text{GW}}(t, k)}{\rho_{\text{tot}}(t)}. \quad (\text{A.14})$$

The present value of Ω_{GW} may be decomposed as follows

$$\Omega_{\text{GW}}(t_0, k) = \frac{\rho_{\text{GW}}(t_0, k)}{\rho_{\text{GW}}(t_{\text{hi}}, k)} \frac{\rho_{\text{GW}}(t_{\text{hi}}, k)}{\rho_{\text{r}}(t_{\text{hi}})} \frac{\rho_{\text{r}}(t_{\text{hi}})}{\rho_{\text{r}}(t_0)} \frac{\rho_{\text{r}}(t_0)}{\rho_{\text{tot}}(t_0)}. \quad (\text{A.15})$$

Assuming that no significant entropy injection has occurred between the time of horizon entry for GWs with wavenumber k and the matter-radiation equality, we obtain

$$\frac{\rho_{\text{GW}}(t_0, k)}{\rho_{\text{GW}}(t_{\text{hi}}, k)} \simeq \left(\frac{a_{\text{hi}}}{a_0}\right)^4, \quad (\text{A.16})$$

$$\frac{\rho_{\text{GW}}(t_{\text{hi}}, k)}{\rho_{\text{r}}(t_{\text{hi}})} = \frac{1}{64\pi G} \frac{k^2}{a_{\text{hi}}^2} \Delta_{\text{GW,prim}}^2(k) \frac{1}{\rho_{\text{r,hi}}} = \frac{1}{24} \Delta_{\text{GW,prim}}^2(k_0) \left(\frac{k}{k_0}\right)^{n_t}, \quad (\text{A.17})$$

$$\frac{\rho_{\text{r}}(t_{\text{hi}})}{\rho_{\text{r}}(t_0)} = \frac{\frac{\pi^2}{30} g_*(T_{\text{hi}}) T_{\text{hi}}^4}{\frac{\pi^2}{30} g_*(T_0) T_0^4} = \left(\frac{g_*(T_{\text{hi}})}{g_*(T_{\text{eq}})}\right) \left(\frac{g_{*s}(T_{\text{eq}}) a_0^3}{g_{*s}(T_{\text{hi}}) a_{\text{hi}}^3}\right)^{4/3}, \quad (\text{A.18})$$

$$\frac{\rho_{\text{r}}(t_0)}{\rho_{\text{tot}}(t_0)} = \Omega_{\text{r},0}, \quad (\text{A.19})$$

where $\Omega_{\text{r},0}$ and $g_*(T_0)$ are defined as if all neutrinos would be relativistic: $g_*(T_0) = g_*(T_{\text{eq}})$. The final numerical result does not depend on this definition. See also Ref. [55]. With the tensor-to-scalar ratio r , which is defined as

$$r \equiv \frac{\Delta_{\text{GW,prim}}^2(k_0)}{\Delta_{\mathcal{R},\text{prim}}^2(k_0)}, \quad (\text{A.20})$$

where $\Delta_{\mathcal{R},\text{prim}}^2$ is the dimensionless power spectrum of curvature perturbation \mathcal{R} , Ω_{GW} becomes

$$\Omega_{\text{GW}}(t_0, k) = \frac{r}{24} \Omega_{\text{r},0} \Delta_{\mathcal{R},\text{prim}}^2(k_0) \left(\frac{k}{k_0}\right)^{n_t} \left(\frac{g_*(T_{\text{hi}})}{g_*(T_{\text{eq}})}\right) \left(\frac{g_{*s}(T_{\text{eq}})}{g_{*s}(T_{\text{hi}})}\right)^{4/3}. \quad (\text{A.21})$$

Substituting the observed values of the radiation fraction $\Omega_{\text{r},0} \simeq 8.55 \times 10^{-5} [g_*(T_{\text{eq}})/g_*(T_{\text{eq}})^{(\text{std})}]$ and the magnitude of the primordial curvature perturbation $\Delta_{\mathcal{R},\text{prim}}^2(k_0) \simeq 2.22 \times 10^{-9}$ [39], one obtains the expression for the present GW spectrum:

$$\Omega_{\text{GW}}(t_0, k) \simeq 7.9 \times 10^{-15} \left(\frac{g_*(T_{\text{hi}})}{g_*(T_{\text{eq}})^{(\text{std})}}\right) \left(\frac{g_{*s}(T_{\text{eq}})}{g_{*s}(T_{\text{hi}})}\right)^{4/3} \left(\frac{k}{k_0}\right)^{n_t} r. \quad (\text{A.22})$$

In the MSSM, it becomes

$$\Omega_{\text{GW}}^{(\text{std})}(t_0, k) \simeq 2.3 \times 10^{-15} \left(\frac{228.75}{g_{*s}(T_{\text{hi}})}\right)^{1/3} \left(\frac{k}{k_0}\right)^{n_t} r. \quad (\text{A.23})$$

Note that the GW spectrum is almost flat except for the weak dependence on k coming from $T_{\text{hi}}(k)$ and the tensor spectral index n_t as long as the corresponding modes k enter the horizon at the RD era.

For completeness, we also present the GW spectrum for the long wavelength modes entering the horizon at the MD era:

$$\Omega_{\text{GW}}(t_0, k) = \frac{r}{12} \Omega_{\text{m},0}^2 \left(\frac{9H_0^2}{32k^2}\right) \Delta_{\mathcal{R},\text{prim}}^2(k_0) \left(\frac{k}{k_0}\right)^{n_t}, \quad (\text{A.24})$$

where $\Omega_{m,0}$ is the density parameter of the matter at present. By using $k_{\text{eq}} = a_{\text{eq}}H_{\text{eq}} = \sqrt{2}\Omega_{m,0}H_0/\sqrt{\Omega_{r,0}} = 0.073\Omega_{m,0}h^2\text{Mpc}^{-1}$, we thus obtain the interpolation formula from $k \ll k_{\text{eq}}$ to $k \gg k_{\text{eq}}$ as

$$\Omega_{\text{GW}}(t_0, k) \simeq \Omega_{\text{GW}}(t_0, k \ll k_{\text{eq}}) \left(\frac{g_*(T_{\text{hi}})}{g_*(T_{\text{eq}})} \right) \left(\frac{g_{*s}(T_{\text{eq}})}{g_{*s}(T_{\text{hi}})} \right)^{4/3} \left(1 + \frac{32k^2}{9k_{\text{eq}}^2} \right), \quad (\text{A.25})$$

which is equivalent to the expression given e.g. in Ref. [9, 13].

B GW spectrum with a brief period of inflation

In this section we derive the GW spectrum with a brief period of thermal inflation.

B.1 GW spectrum with brief period of inflation

First note that if the universe is dominated by some matter whose equation of state is w , the total energy density and the Hubble parameter evolves as

$$\rho_{\text{tot}}(t) \propto a(t)^{-3(1+w)} \rightarrow H \propto a(t)^{-3(1+w)/2}. \quad (\text{B.1})$$

Therefore, the scale factor at which the mode with wavenumber k enters the horizon is given by

$$k = a_{\text{in}}(k)H_{\text{in}}(k) \rightarrow a_{\text{in}}(k) \propto k^{-2/(1+3w)} \quad \text{for } w > -1/3. \quad (\text{B.2})$$

For $w < -1/3$, the mode exits the horizon at

$$k = a_{\text{out}}(k)H_{\text{out}}(k) \rightarrow a_{\text{out}}(k) \propto k^{-2/(1+3w)} \quad \text{for } w < -1/3. \quad (\text{B.3})$$

Now let us consider the case where the equation of state changes as $w_1 \rightarrow w_2 \rightarrow w_3$ with $w_1, w_3 > -1/3$ and $w_2 < -1/3$ as in the case of thermal inflation (see Fig. 17). We want to evaluate the GW spectrum at late time $t \gg t_3$.

(i) $k < k_d$: In the long-wavelength limit, we obtain

$$\rho_{\text{GW}}(k, t) \propto \rho_{\text{GW,prim}}(k, t_i) \times \left(\frac{a(t_i)}{a_{\text{in}}(k)} \right)^2 \left(\frac{a_{\text{in}}(k)}{a(t)} \right)^4 \propto \rho_{\text{GW,prim}}(k) \times k^{-4/(1+3w_3)}. \quad (\text{B.4})$$

Here

$$\rho_{\text{GW,prim}}(k, t_i) \equiv \frac{1}{32\pi G} \frac{k^2}{a(t_i)^2} \Delta_{\text{GW,prim}}^2(k). \quad (\text{B.5})$$

(ii) $k_d < k < k_{\text{PT}}$: In this case, the mode experiences the horizon entry and horizon exit, and again enters the horizon. First, the spectrum at $t = t_2$ is given by

$$\rho_{\text{GW}}(k, t_2) \propto \rho_{\text{GW,prim}}(k, t_i) \times \left(\frac{a(t_i)}{a_{\text{in}}(k)} \right)^2 \left(\frac{a_{\text{in}}(k)}{a(t_2)} \right)^4 \propto \rho_{\text{GW,prim}}(k) \times k^{-4/(1+3w_1)}, \quad (\text{B.6})$$

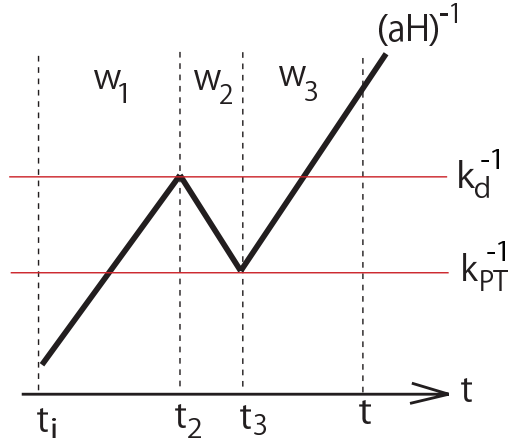


Figure 17: Schematic picture for the evolution of the Hubble radius.

Next, at $t = t_3$ it becomes

$$\rho_{\text{GW}}(k, t_3) \propto \rho_{\text{GW}}(k, t_2) \times \left(\frac{a(t_2)}{a_{\text{out}}(k)} \right)^4 \left(\frac{a_{\text{out}}(k)}{a(t_3)} \right)^2 \propto \rho_{\text{GW}}(k, t_2) \times k^{4/(1+3w_2)}, \quad (\text{B.7})$$

Finally, at late time t , we have

$$\rho_{\text{GW}}(k, t) \propto \rho_{\text{GW}}(k, t_3) \times \left(\frac{a(t_3)}{a_{\text{in}}(k)} \right)^2 \left(\frac{a_{\text{in}}(k)}{a(t)} \right)^4 \propto \rho_{\text{GW}}(k, t_3) \times k^{-4/(1+3w_3)}, \quad (\text{B.8})$$

In summary,

$$\rho_{\text{GW}}(k, t) \propto \rho_{\text{GW,prim}}(k) \times k^{-4/(1+3w_1)} k^{4/(1+3w_2)} k^{-4/(1+3w_3)}, \quad (\text{B.9})$$

(iii) $k > k_{\text{PT}}$: In the short-wavelength limit, we obtain

$$\rho_{\text{GW}}(k, t) \propto \rho_{\text{GW,prim}}(k, t_i) \times \left(\frac{a(t_i)}{a_{\text{in}}(k)} \right)^2 \left(\frac{a_{\text{in}}(k)}{a(t)} \right)^4 \propto \rho_{\text{GW,prim}}(k) \times k^{-4/(1+3w_1)}. \quad (\text{B.10})$$

Collecting the above results, we finally arrive at

$$\rho_{\text{GW}}(k, t) \propto \begin{cases} \rho_{\text{GW,prim}}(k) \times k^{-4/(1+3w_3)} & \text{for } k < k_d \\ \rho_{\text{GW,prim}}(k) \times k^{-4/(1+3w_1)} k^{4/(1+3w_2)} k^{-4/(1+3w_3)} & \text{for } k_d < k < k_{\text{PT}} \\ \rho_{\text{GW,prim}}(k) \times k^{-4/(1+3w_1)} & \text{for } k > k_{\text{PT}} \end{cases} \quad (\text{B.11})$$

Note that $\rho_{\text{GW,prim}}(k) \propto k^2$. Here k_d and k_{PT} are the comoving Hubble scale at the beginning of thermal inflation and that at the end of thermal inflation (or at the phase transition),

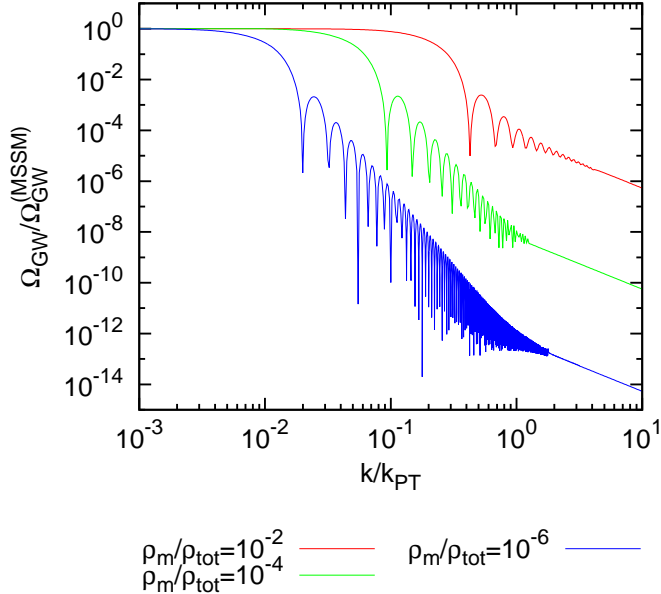


Figure 18: GW spectrum with phase transition and instant decay into radiation. We assumed that the universe is matter dominated before the vacuum energy dominates it, and varied the ratio of matter energy density to the total energy density at the phase transition.

respectively (see Fig. 17). Thus in the case of $w_1 = w_3 = 1/3$ and $w_2 = -1$, we obtain the GW spectrum

$$\Omega_{\text{GW}}(t_0, k) = \Omega_{\text{GW}}^{(\text{std})}(t_0, k) \times \begin{cases} 1 & \text{for } k < k_d \\ (k_d/k)^4 & \text{for } k_d < k < k_{\text{PT}} \\ (k_d/k_{\text{PT}})^4 & \text{for } k > k_{\text{PT}} \end{cases} . \quad (\text{B.12})$$

Therefore, in the intermediate frequency region, the spectrum is proportional to k^{-4} (see Fig. 3). Similarly, for $w_1 = 0, w_3 = 1/3$ and $w_2 = -1$, we have $\Omega_{\text{GW}}(t_0, k) \propto k^{-6}$ for $k_d < k < k_{\text{PT}}$. Fig. 18 shows the GW spectrum for the case where the universe is matter dominated before thermal inflation and the vacuum energy instantly goes to radiation after the phase transition, with varying the ratio of matter energy density to the vacuum energy at the phase transition. It is seen that the spectrum scales as k^{-6} for $k_d < k < k_{\text{PT}}$.

Although the above arguments give global picture of the GW spectral shape, actually there appear an oscillatory feature in the GW spectrum for $k_d < k < k_{\text{PT}}$, which is not seen for $k < k_d$ and $k > k_{\text{PT}}$ (see e.g., Fig. 3). Below we see more detail on the oscillatory feature of the GW spectrum.

B.2 Oscillations in the GW spectrum

As shown in Fig. 3, the GW spectrum has typical oscillations in the case of brief period of thermal inflation. Here we see the reason for such a behavior and derive the oscillation

period.

B.2.1 The reason for the oscillations in the GW spectrum

The GW with modes $k_d < k < k_{\text{PT}}$ experience additional “horizon exit” and “horizon entry” processes compared with other modes (see Fig. 17). Let us denote the value of $h(t, k, \lambda)$ and its time derivative at this horizon exit by $h(t_{\text{ex}}, k, \lambda)$ and $\dot{h}(t_{\text{ex}}, k, \lambda)$. Note that, although they take different values for different k since they are oscillating, the combination $[\dot{h}(t_{\text{ex}}, k, \lambda)]^2 + (k/a)^2[h(t_{\text{ex}}, k, \lambda)]^2$ is roughly the same for different k . After the horizon exit, the equation of motion of GWs is approximated by

$$\ddot{h}(t, k, \lambda) + 3H\dot{h}(t, k, \lambda) = 0, \quad (\text{B.13})$$

the general solution of which is given by

$$h(t, k, \lambda) = H_1 + H_2 e^{-3Ht}, \quad (\text{B.14})$$

where coefficients H_1 and H_2 are determined by the boundary condition at the horizon exit. Then we find

$$h(t, k, \lambda) = \left(h(t_{\text{ex}}, k, \lambda) + \frac{1}{3H} \dot{h}(t_{\text{ex}}, k, \lambda) \right) - \frac{1}{3H} \dot{h}(t_{\text{ex}}, k, \lambda) e^{-3H(t-t_{\text{ex}})}, \quad (\text{B.15})$$

$$\dot{h}(t, k, \lambda) = \dot{h}(t_{\text{ex}}, k, \lambda) e^{-3H(t-t_{\text{ex}})}. \quad (\text{B.16})$$

Therefore the part of the GW energy density proportional to \dot{h}^2 at the horizon exit soon damps. The modes with $\dot{h}(t_{\text{ex}}, k, \lambda) = 0$ appear to be peaks in the GW spectrum. On the other hand, the modes satisfying $h(t_{\text{ex}}, k, \lambda) + \dot{h}(t_{\text{ex}}, k, \lambda)/3H = 0$ give troughs in the GW spectrum. Thus we expect oscillatory features in the GW spectrum for $k_d < k < k_{\text{PT}}$ in the case of thermal inflation.

B.2.2 Oscillation period

Now we calculate the oscillation period in the GW spectrum. We see that the oscillation period reflects the state of the universe before thermal inflation.

First we consider the case where the universe was RD dominated before thermal inflation. We solve the Friedmann equation

$$H^2 = \frac{8\pi G}{3} \left[\rho_{\text{r,ref}} \left(\frac{a_{\text{ref}}}{a} \right)^4 + \rho_{\text{vac}} \right], \quad (\text{B.17})$$

where the subscript “ref” denotes some reference time before the phase transition, to get

$$\frac{a}{a_{\text{ref}}} = \left(\frac{\rho_{\text{r,ref}}}{\rho_{\text{vac}}} \right)^{1/4} \sinh^{1/2}(2\omega_{\text{RD}} t), \quad (\text{B.18})$$

where

$$\omega_{\text{RD}} = \left(\frac{8\pi G}{3} \rho_{\text{vac}} \right)^{1/2} \simeq H_{\text{PT}}. \quad (\text{B.19})$$

Here we have assumed that the inflation diluted the radiation enough. In the following we consider GWs which are well-inside around the vacuum-energy domination and well-outside the horizon at the phase transition. The variable $u \equiv k \int_0^t dt'/a(t')$ at the phase transition is

$$\begin{aligned} u_{\text{PT}} &= k \int_0^{t_{\text{PT}}} \frac{dt}{a} \\ &\simeq \frac{1}{2} \frac{k}{a_{\text{PT}} \omega_{\text{RD}}} \left[\frac{\rho_{\text{vac}}}{(a_{\text{ref}}/a_{\text{PT}})^4 \rho_{\text{r,ref}}} \right]^{1/4} \int_0^\infty \frac{dx}{(1+x^2)^{1/2} x^{1/2}} \\ &\simeq \frac{1}{2} \frac{k}{a_{\text{PT}} H_{\text{PT}}} f_{\text{r,PT}}^{-1/4} \int_0^\infty \frac{dx}{(1+x^2)^{1/2} x^{1/2}}, \end{aligned} \quad (\text{B.20})$$

where $x = \sinh(2\omega_{\text{RD}}t)$ and $f_{\text{r,PT}} \equiv \rho_{\text{r,PT}}/\rho_{\text{tot}}$ is the energy fraction of radiation at the phase transition. The oscillation peaks appear with the period of π in u_{PT} ,^{#11} therefore the gap between two neighboring peaks is

$$\Delta u_{\text{PT}} = \frac{1}{2} \frac{\Delta k}{a_{\text{PT}} H_{\text{PT}}} f_{\text{r,PT}}^{-1/4} \int_0^1 \frac{dx}{(1+x^2)^{1/2} x^{1/2}} = \pi. \quad (\text{B.21})$$

From this equation and $k_{\text{PT}} \equiv a_{\text{PT}} H_{\text{PT}}$ we obtain

$$\frac{\Delta k}{k_{\text{PT}}} \simeq \frac{\pi}{1.854} f_{\text{r,PT}}^{1/4} \quad (\text{B.22})$$

In the case of MD universe before thermal inflation, we follow the same procedure. Solving the Friedmann equation

$$H^2 = \frac{8\pi G}{3} \left[\rho_{\text{m,ref}} \left(\frac{a_{\text{ref}}}{a} \right)^3 + \rho_{\text{vac}} \right], \quad (\text{B.23})$$

^{#11} As mentioned before, h with wavenumbers of our interest goes out of the horizon during thermal inflation. One of the two solution to the equation of motion of GWs soon damp outside the horizon (see the previous subsection), and the peaks in the GW spectrum correspond to those wavenumbers which give maximal H_1 in Eq. (B.14). Such wavenumbers appear with period π in terms of u_{he} (Here we denote ‘‘horizon exit’’ by ‘‘he’’). The point is that u_{he} is almost the same as u_{PT} , since by the same calculation as Eq. (B.20) we find

$$u_{\text{he}} = k \int_0^{t_{\text{he}}} \frac{dt}{a} = \frac{1}{2} \frac{k}{a_{\text{PT}} H_{\text{PT}}} f_{\text{r,PT}}^{-1/4} \int_0^{x_{\text{he}}} \frac{dx}{(1+x^2)^{1/2} x^{1/2}},$$

with x_{he} given by

$$k = a_{\text{he}} H_{\text{he}} \leftrightarrow \left(x_{\text{he}} + \frac{1}{x_{\text{he}}} \right)^{1/2} \simeq \frac{k}{a_{\text{PT}} H_{\text{PT}}} \left(\frac{\rho_{\text{vac}}}{\rho_{\text{r,PT}}} \right)^{1/4}.$$

One finds $x_{\text{he}} \gg 1$ because both of the two factors $k/a_{\text{PT}} H_{\text{PT}}$ and $(\rho_{\text{vac}}/\rho_{\text{r,PT}})^{1/4}$ are much larger than 1. Note that $k/a_{\text{PT}} H_{\text{PT}} \gg 1$ although the GWs are out of horizon at the phase transition.

we get

$$\frac{a}{a_{\text{ref}}} = \left(\frac{\rho_{\text{m,ref}}}{\rho_{\text{vac}}} \right)^{1/3} \sinh^{2/3}(2\omega_{\text{MD}}t), \quad (\text{B.24})$$

where

$$\omega_{\text{MD}} = \frac{3}{4} \left(\frac{8\pi G}{3} \rho_{\text{vac}} \right)^{1/2} \simeq \frac{3}{4} H_{\text{PT}}. \quad (\text{B.25})$$

Then we get

$$\begin{aligned} u_{\text{PT}} &= k \int_0^{t_{\text{PT}}} \frac{dt'}{a} \\ &\simeq \frac{1}{2} \frac{k}{a_{\text{PT}} \omega_{\text{MD}}} \left[\frac{\rho_{\text{vac}}}{(a_{\text{ref}}/a_{\text{PT}})^3 \rho_{\text{m,ref}}} \right]^{1/3} \int_0^\infty \frac{dx}{(1+x^2)^{1/2} x^{2/3}} \\ &\simeq \frac{2}{3} \frac{k}{a_{\text{PT}} H_{\text{PT}}} f_{\text{m,PT}}^{-1/3} \int_0^\infty \frac{dx}{(1+x^2)^{1/2} x^{2/3}}, \end{aligned} \quad (\text{B.26})$$

and

$$\frac{\Delta k}{k_{\text{PT}}} \simeq \frac{\pi}{2.804} f_{\text{m,PT}}^{1/3}, \quad (\text{B.27})$$

where $f_{\text{m,PT}}$ is the energy fraction of matter at the phase transition.

References

- [1] M. S. Turner and F. Wilczek, Phys. Rev. Lett. **65**, 3080 (1990).
- [2] N. Seto and J. 'I. Yokoyama, J. Phys. Soc. Jap. **72**, 3082 (2003) [gr-qc/0305096].
- [3] H. Tashiro, T. Chiba and M. Sasaki, Class. Quant. Grav. **21**, 1761 (2004) [gr-qc/0307068].
- [4] L. A. Boyle and P. J. Steinhardt, Phys. Rev. D **77**, 063504 (2008) [astro-ph/0512014].
- [5] L. A. Boyle and A. Buonanno, Phys. Rev. D **78**, 043531 (2008) [arXiv:0708.2279 [astro-ph]].
- [6] K. Nakayama, S. Saito, Y. Suwa and J. 'i. Yokoyama, Phys. Rev. D **77**, 124001 (2008) [arXiv:0802.2452 [hep-ph]].
- [7] K. Nakayama, S. Saito, Y. Suwa and J. 'i. Yokoyama, JCAP **0806**, 020 (2008) [arXiv:0804.1827 [astro-ph]].

- [8] S. Kuroyanagi, T. Chiba and N. Sugiyama, Phys. Rev. D **79**, 103501 (2009) [arXiv:0804.3249 [astro-ph]].
- [9] K. Nakayama and J. 'i. Yokoyama, JCAP **1001**, 010 (2010) [arXiv:0910.0715 [astro-ph.CO]].
- [10] K. Nakayama and F. Takahashi, JCAP **1011**, 009 (2010) [arXiv:1008.2956 [hep-ph]].
- [11] S. Schettler, T. Boeckel and J. Schaffner-Bielich, Phys. Rev. D **83**, 064030 (2011) [arXiv:1010.4857 [astro-ph.CO]].
- [12] R. Durrer and J. Hasenkamp, Phys. Rev. D **84**, 064027 (2011) [arXiv:1105.5283 [gr-qc]].
- [13] S. Kuroyanagi, K. Nakayama and S. Saito, Phys. Rev. D **84**, 123513 (2011) [arXiv:1110.4169 [astro-ph.CO]].
- [14] R. Saito and S. Shirai, Phys. Lett. B **713**, 237 (2012) [arXiv:1201.6589 [hep-ph]].
- [15] N. Seto, S. Kawamura and T. Nakamura, Phys. Rev. Lett. **87**, 221103 (2001) [astro-ph/0108011]; S. Kawamura *et al.*, Class. Quant. Grav. **28**, 094011 (2011).
- [16] J. Crowder and N. J. Cornish, Phys. Rev. D **72**, 083005 (2005) [gr-qc/0506015].
- [17] C. Cutler and D. E. Holz, Phys. Rev. D **80**, 104009 (2009) [arXiv:0906.3752 [astro-ph.CO]].
- [18] K. Yamamoto, Phys. Lett. B **168**, 341 (1986); G. Lazarides, C. Panagiotakopoulos and Q. Shafi, Phys. Rev. Lett. **56**, 557 (1986).
- [19] D. H. Lyth and E. D. Stewart, Phys. Rev. Lett. **75**, 201 (1995) [hep-ph/9502417]; Phys. Rev. D **53**, 1784 (1996) [hep-ph/9510204].
- [20] R. Jinno, T. Moroi and K. Nakayama, Phys. Lett. B **713**, 129 (2012) [arXiv:1112.0084 [hep-ph]].
- [21] S. Weinberg, Phys. Rev. D **69**, 023503 (2004) [astro-ph/0306304].
- [22] D. A. Dicus and W. W. Repko, Phys. Rev. D **72**, 088302 (2005) [astro-ph/0509096].
- [23] Y. Watanabe and E. Komatsu, Phys. Rev. D **73**, 123515 (2006) [astro-ph/0604176].
- [24] K. Ichiki, M. Yamaguchi and J. 'I. Yokoyama, Phys. Rev. D **75**, 084017 (2007) [hep-ph/0611121].
- [25] R. Jinno, T. Moroi and K. Nakayama, Phys. Rev. D **86**, 123502 (2012) [arXiv:1208.0184 [astro-ph.CO]].
- [26] R. D. Peccei and H. R. Quinn, Phys. Rev. Lett. **38**, 1440 (1977).

- [27] For reviews, see J. E. Kim, Phys. Rept. **150**, 1 (1987); J. E. Kim and G. Carosi, Rev. Mod. Phys. **82**, 557 (2010) [arXiv:0807.3125 [hep-ph]].
- [28] For a review, see M. Kawasaki and K. Nakayama, arXiv:1301.1123 [hep-ph].
- [29] T. Hiramatsu, M. Kawasaki and K. i. Saikawa, JCAP **1108**, 030 (2011) [arXiv:1012.4558 [astro-ph.CO]]; T. Hiramatsu, M. Kawasaki, K. i. Saikawa and T. Sekiguchi, Phys. Rev. D **85**, 105020 (2012) [Erratum-ibid. D **86**, 089902 (2012)] [arXiv:1202.5851 [hep-ph]]; JCAP **1301**, 001 (2013) [arXiv:1207.3166 [hep-ph]].
- [30] M. Kawasaki, N. Kitajima and K. Nakayama, Phys. Rev. D **82**, 123531 (2010) [arXiv:1008.5013 [hep-ph]]; Phys. Rev. D **83**, 123521 (2011) [arXiv:1104.1262 [hep-ph]].
- [31] T. Moroi and M. Takimoto, Phys. Lett. B **718**, 105 (2012) [arXiv:1207.4858 [hep-ph]].
- [32] T. Moroi, K. Mukaida, K. Nakayama and M. Takimoto, JHEP **1306** (2013) 040 [arXiv:1304.6597 [hep-ph]].
- [33] A. Anisimov and M. Dine, Nucl. Phys. B **619**, 729 (2001) [hep-ph/0008058].
- [34] M. Laine, Prog. Theor. Phys. Suppl. **186**, 404 (2010) [arXiv:1007.2590 [hep-ph]].
- [35] Y. Chikashige, R. N. Mohapatra and R. D. Peccei, Phys. Lett. B **98**, 265 (1981).
- [36] E. J. Chun, H. B. Kim and A. Lukas, Phys. Lett. B **328**, 346 (1994) [hep-ph/9403217].
- [37] T. Yanagida, in Proceedings of the “*Workshop on the Unified Theory and the Baryon Number in the Universe*”, Tsukuba, Japan, Feb. 13-14, 1979, edited by O. Sawada and A. Sugamoto, KEK report KEK-79-18, p. 95, and “*Horizontal Symmetry And Masses Of Neutrinos*”, Prog. Theor. Phys. **64** (1980) 1103; M. Gell-Mann, P. Ramond and R. Slansky, in “*Supergravity*” (North-Holland, Amsterdam, 1979) eds. D. Z. Freedman and P. van Nieuwenhuizen, Print-80-0576 (CERN); see also P. Minkowski, Phys. Lett. B **67**, 421 (1977).
- [38] For a review, see M. Maggiore, Phys. Rept. **331**, 283 (2000) [gr-qc/9909001].
- [39] P. A. R. Ade *et al.* [Planck Collaboration], arXiv:1303.5076 [astro-ph.CO].
- [40] D. Croon, J. Ellis and N. E. Mavromatos, arXiv:1303.6253 [astro-ph.CO].
- [41] K. Nakayama, F. Takahashi and T. T. Yanagida, arXiv:1303.7315 [hep-ph]; arXiv:1305.5099 [hep-ph].
- [42] A. D. Linde, Phys. Lett. B **132**, 317 (1983); C. Destri, H. J. de Vega and N. G. Sanchez, Phys. Rev. D **77**, 043509 (2008) [astro-ph/0703417]; R. Kallosh and A. D. Linde, JCAP **0704**, 017 (2007) [arXiv:0704.0647 [hep-th]].

- [43] F. L. Bezrukov and M. Shaposhnikov, Phys. Lett. B **659**, 703 (2008) [arXiv:0710.3755 [hep-th]].
- [44] S. Ferrara, R. Kallosh, A. Linde, A. Marrani and A. Van Proeyen, Phys. Rev. D **82**, 045003 (2010) [arXiv:1004.0712 [hep-th]]; Phys. Rev. D **83**, 025008 (2011) [arXiv:1008.2942 [hep-th]].
- [45] R. Kallosh and A. Linde, arXiv:1306.3211 [hep-th].
- [46] C. Germani and A. Kehagias, Phys. Rev. Lett. **105**, 011302 (2010) [arXiv:1003.2635 [hep-ph]].
- [47] K. Nakayama and F. Takahashi, JCAP **1102**, 010 (2011) [arXiv:1008.4457 [hep-ph]].
- [48] K. Kamada, T. Kobayashi, T. Takahashi, M. Yamaguchi and J. 'i. Yokoyama, Phys. Rev. D **86**, 023504 (2012) [arXiv:1203.4059 [hep-ph]].
- [49] A. A. Starobinsky, Phys. Lett. B **91**, 99 (1980).
- [50] J. Ellis, D. V. Nanopoulos and K. A. Olive, arXiv:1305.1247 [hep-th].
- [51] R. Kallosh and A. Linde, arXiv:1306.3214 [hep-th].
- [52] A. D. Linde, Phys. Lett. B **327**, 208 (1994) [astro-ph/9402031].
- [53] A. Vilenkin, Phys. Rev. Lett. **72**, 3137 (1994) [hep-th/9402085].
- [54] K. Harigaya, M. Kawasaki and T. T. Yanagida, Phys. Lett. B **719**, 126 (2013) [arXiv:1211.1770 [hep-ph]].
- [55] W. Buchmuller, V. Domcke, K. Kamada and K. Schmitz, arXiv:1305.3392 [hep-ph].